

# Comparison and calibration of nonheating paleointensity methods: A case study using dusty olivine

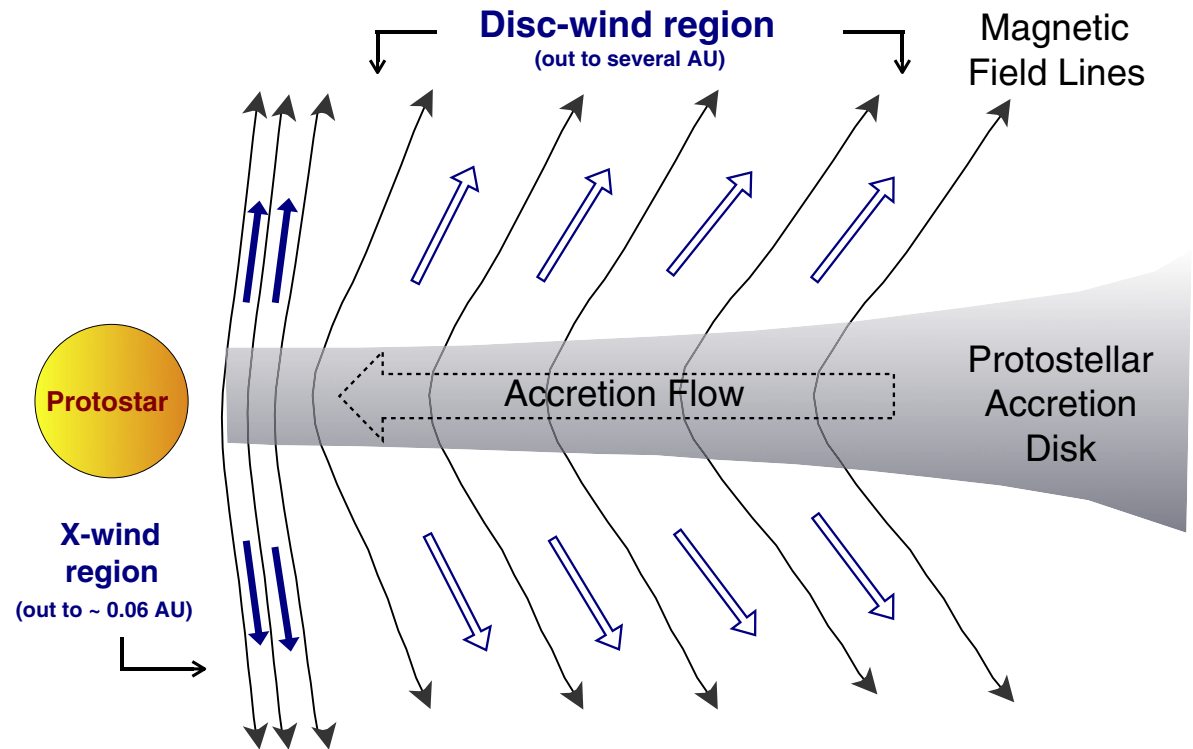
---

Lappe, S.-C. L.L., J. M. Feinberg, A. Muxworthy, and R. J. Harrison (2013), *Geochem. Geophys. Geosyst.*, 14, 2143–2158, doi:10.1002/ggge.20141.

## Chondrule formation

- high temperatures (flash heating)
- different scenarios are associated with different magnetic field intensities
- chondrules may have acquired a pre-accretionary TRM during cooling

→ find a way to reconstruct the field present at chondrule formation by measuring chondritic meteorites



## Dusty olivine

- found in unequilibrated ordinary chondrites

Nagahara H. (1981) **Evidence for secondary origin of chondrules.** *Nature*, 292, 135-136.

- high-Mg olivine grains with  $\mu\text{m}$  to nm sized Fe-Ni inclusions  
→ dusty appearance

Rambaldi, E.R., and J.T. Wasson (1982) **Fine, nickel-poor Fe-Ni grains in the olivine of unequilibrated ordinary chondrites.** *Geochim. Cosmochim. Acta*, 46, 929-939, doi: 10.1016/0016-7037(82)90049-7.

Jones, R.H., and L.R. Danielson (1997) **A chondrule origin for dusty relict olivine in unequilibrated chondrites.** *Meteorit. Planet. Sci.*, 32, 753-760, doi:10.1111/j.1945-5100.1997.tb01565.x.

- formed via sub-solidus reduction of the fayalitic component ( $\text{Fe}_2\text{SiO}_4$ ) of the olivine host crystal during the heating event at the chondrule formation

Boland, J.N., and A. Duba (1981) **Solid-state reduction of iron in olivine - planetary and meteoritic evolution.** *Nature*, 294, 142-144.

# Motivation

---

## Dusty olivine

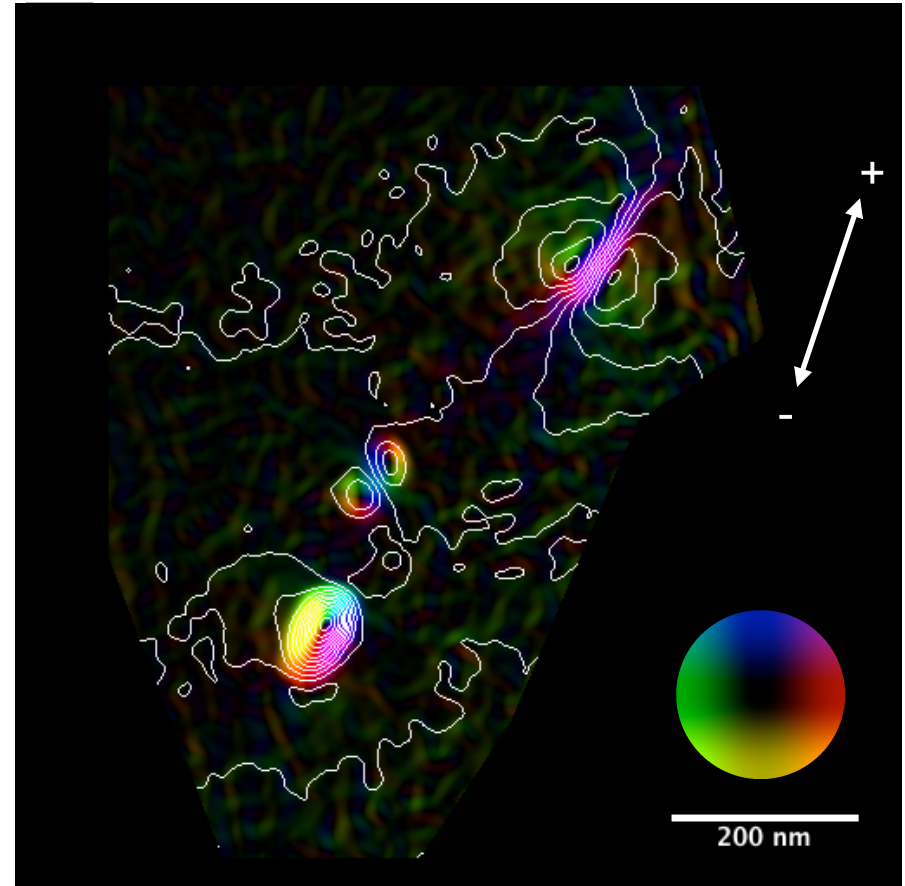
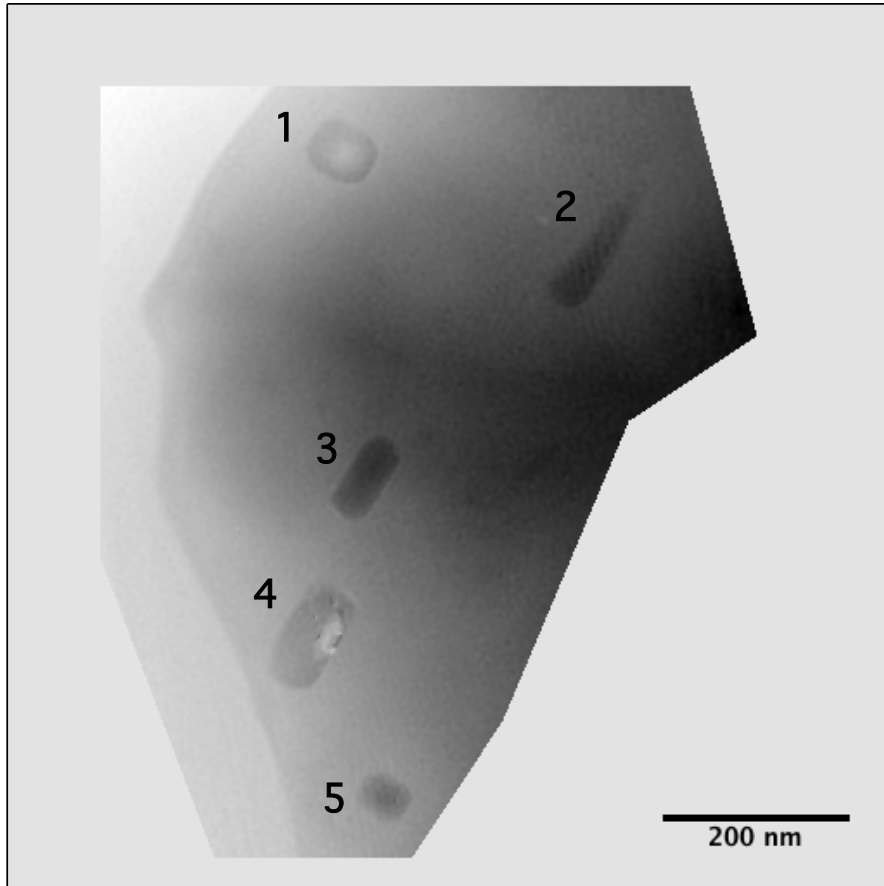
- chondrules cools through the Curie temperature of Fe in the presence of ancient field  
→ dusty inclusions acquire TRM

Do they still retain a primary TRM?

- shielded from thermal and chemical alteration due to surrounding olivine host crystal
- high coercivities, stable remanence behaviour, high mean destructive field  
→ faithful carrier of pre-accretionary remanence  
→ may retain a record of Early Solar System's magnetic field

# Motivation

## Synthetic dusty olivine



Lappe, S.-C. L. L., N. S. Church, T. Kasama, A. B. da Silva Fanta, G. Bromiley, R. E. Dunin-Borkowski, J. M. Feinberg, S. Russell, and R. J. Harrison (2011), **Mineral magnetism of dusty olivine: A credible recorder of pre-accretionary remanence**, *Geochem. Geophys. Geosyst.*, 12, Q12Z35, doi:10.1029/2011GC003811.

## Synthetic dusty olivine

- Non-interacting single domain uniaxial particles with high coercivity
- Simple and well understood mineralogy
- TRM acquired under conditions that can be reproduced in the lab (similar temperature/pressure/oxygen fugacity/cooling rate)
- Sufficient density of remanence carriers to allow sub-mm sampling/measurement (e.g. using scanning magnetic microscopy)
- Stable with respect to chemical alteration/heating (both in nature and lab)

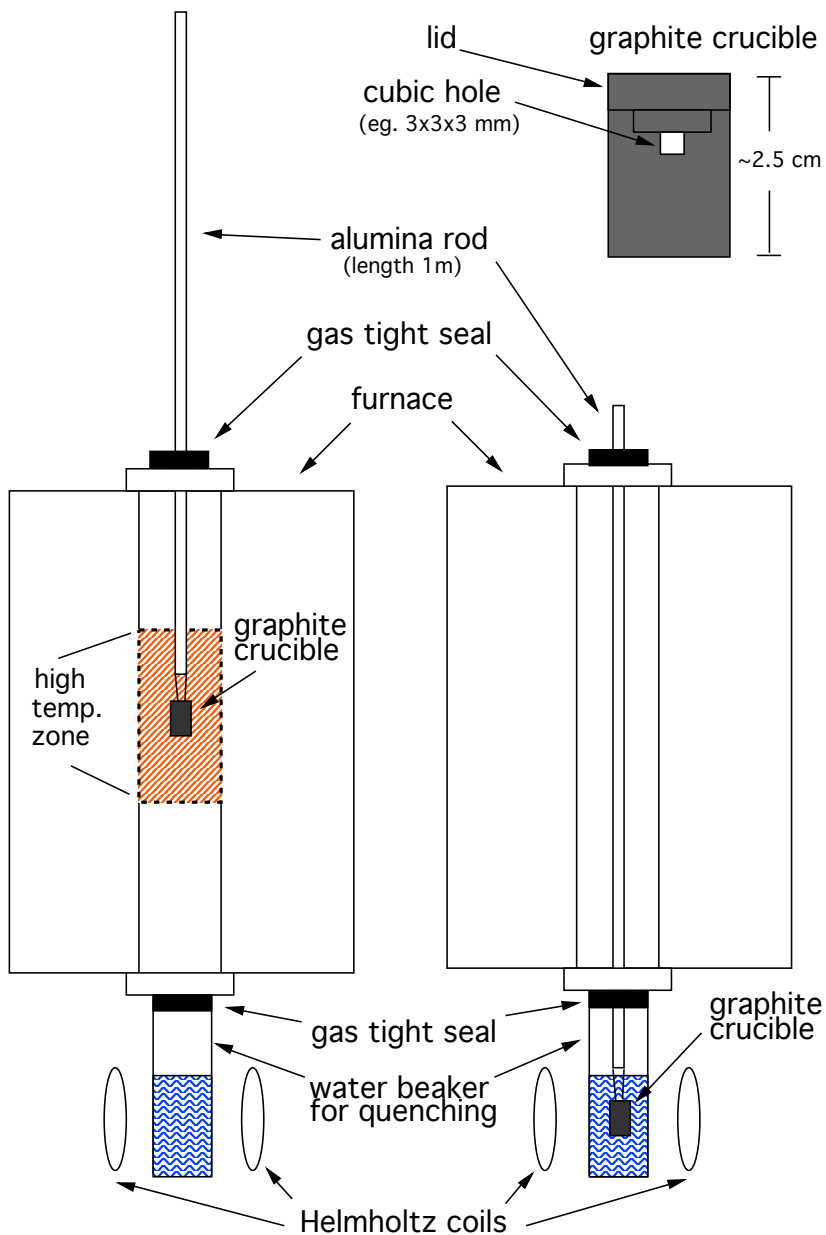
# Motivation

---

Goal: Extract accurate information about the magnetic field intensity, present at the time of chondrule formation, from meteoritic samples

→ establish and calibrate a non-heating method of paleointensity determination

# Sample synthesis



## 3 different starting materials:

- olivine crystals from Icelandic basalt; average comp. 10.2% fayalite; 0.33wt% Ni
- synthetic olivine; 10% fayalite; 0.1wt% Ni
- synthetic olivine; 10% fayalite; Ni-free

## fabrication and characterisation of synthetic olivine:

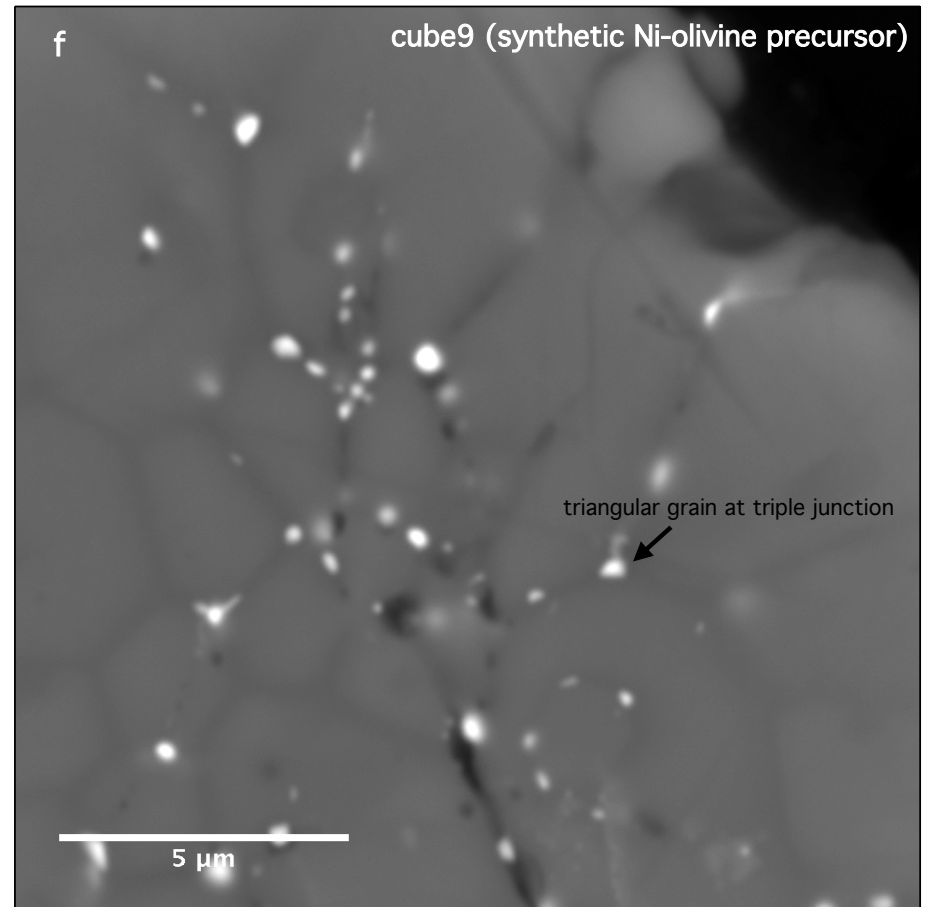
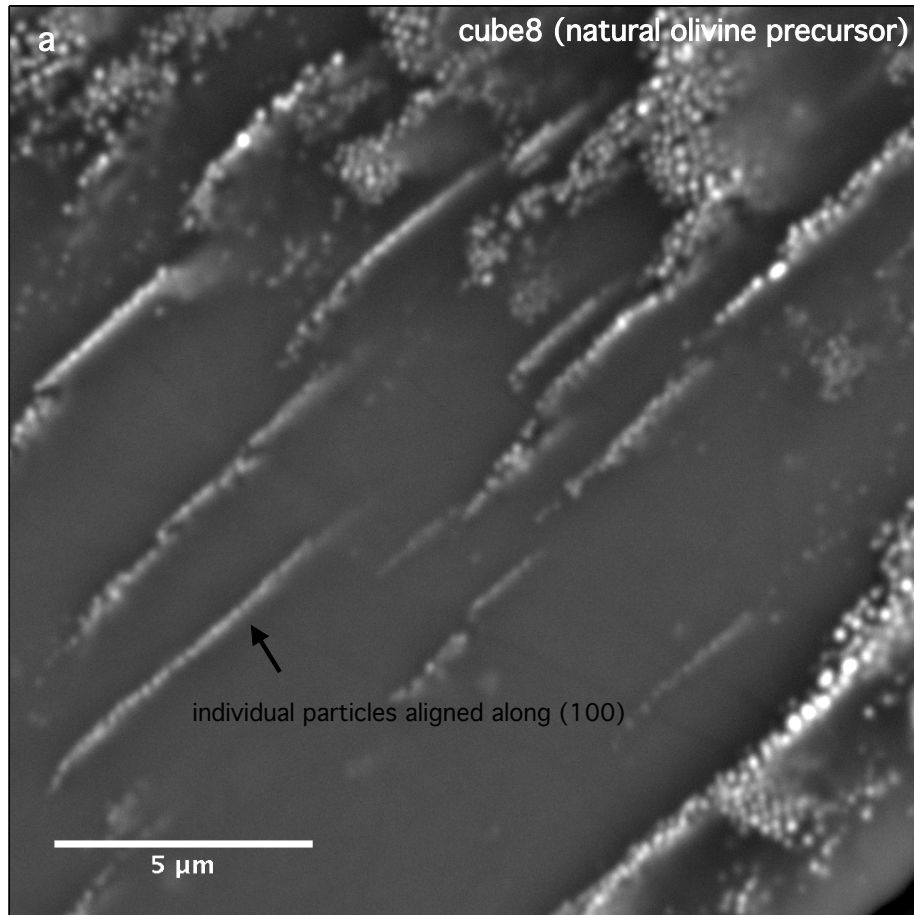
- chemical synthesis from oxides
- X-ray powder diffraction
- SEM
- microprobe

## Samples quenched in a known magnetic field:

- design of unique quenching mechanism
- 6 different fields ranging from 0.2 to 1.5 mT, 2-3 samples each

# Sample characterisation

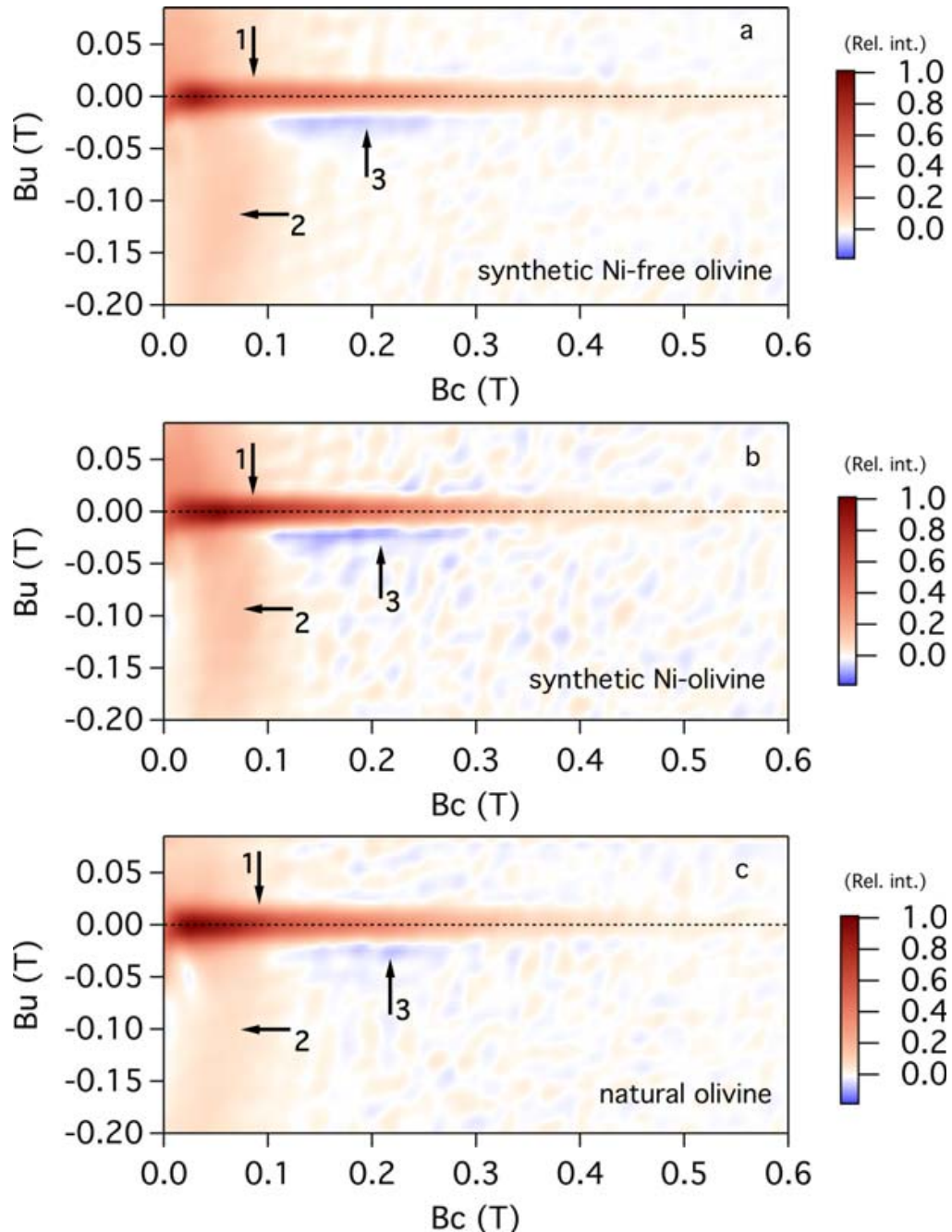
## Microscopy



- all samples resemble natural dusty olivines
- samples made from synthetic olivine show less of the very small Fe-inclusions but seem to contain more particles with irregular shapes and more larger inclusions at grain boundaries

# Sample characterisation

## First-order reversal curve (FORC) measurements



- mix of single domain and vortex states
- coercivity up to 600 mT
- samples made from synthetic olivine generally show higher vortex contribution, i.e. samples made from natural olivine starting material are more SD dominated
- samples made from synthetic olivine also show higher variability in the amount of vortex contribution between different samples
- average vortex annihilation field: 170 mT

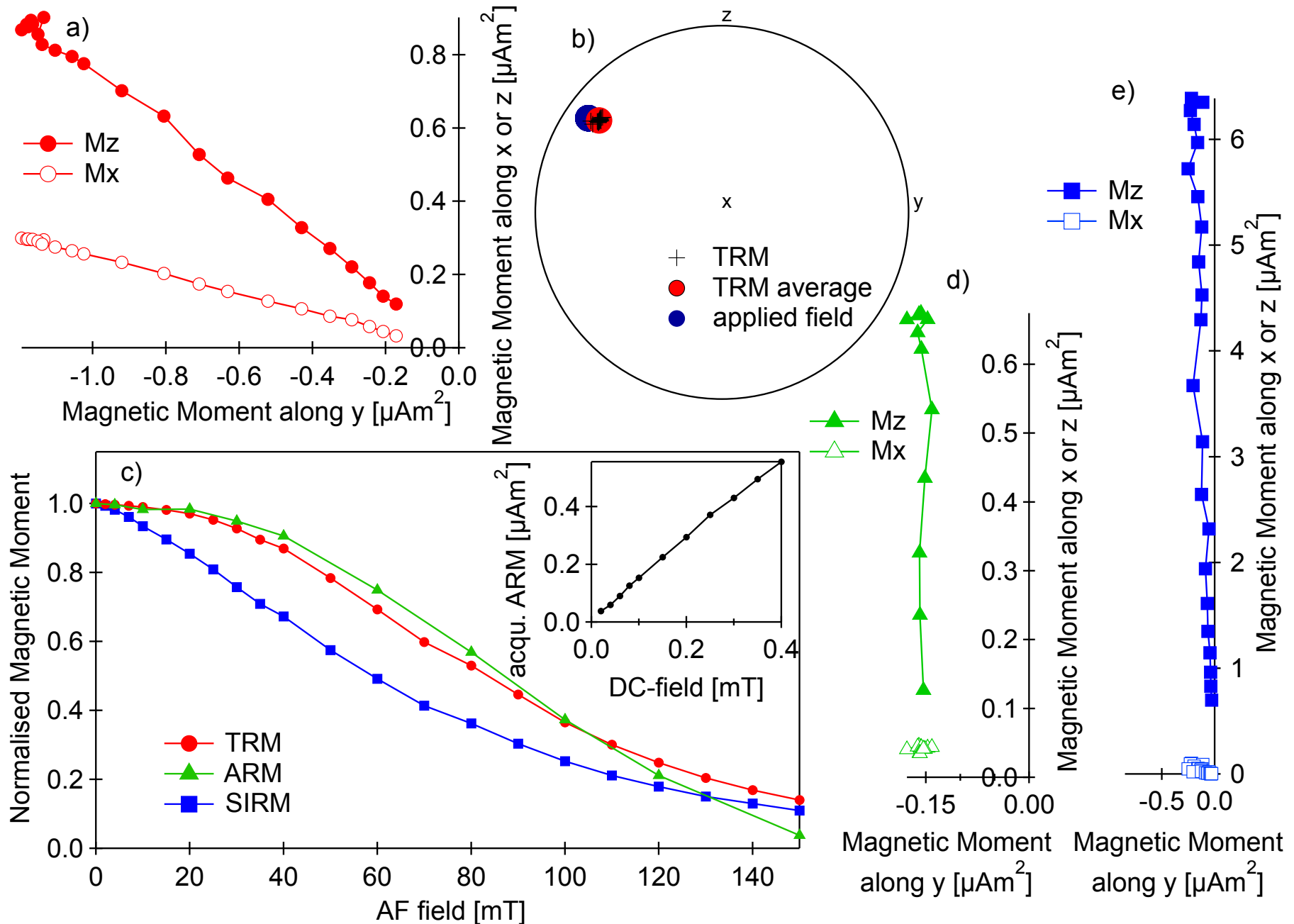
# Rock-magnetic measurements

---

- Alternating-field (AF) demagnetisation of thermoremanent magnetisation (TRM)
- Acquisition of anhysteritic remanent magnetisation (ARM); highest bias field: 0.4 mT
- Alternating-field (AF) demagnetisation of anhysteritic remanent magnetisation (ARM)
- Inducement of saturation isothermal remanent magnetisation (SIRM); applied field: 1T
- Alternating-field (AF) demagnetisation of saturation isothermal remanent magnetisation (SIRM)

# Rock-magnetic measurements

## TRM and IRM demagnetisation, ARM acquisition and demagnetisation

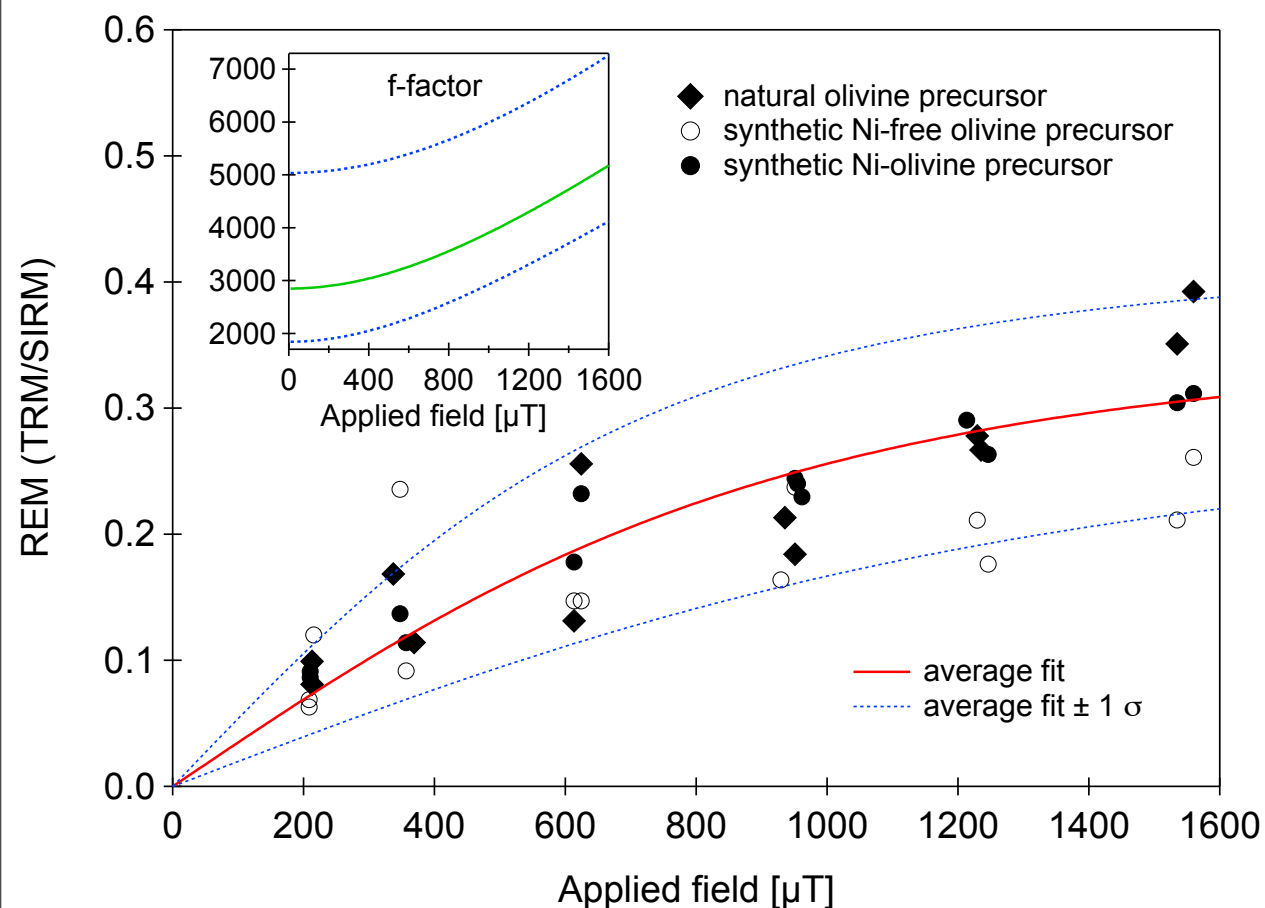


# Rock-magnetic measurements

## Calibration curve relating applied field to recorded remanence: REM

The saturation REM ratio (total TRM/SIRM) shows non-linear behavior as function of applied field, saturating at a value of 0.36. Data were fitted to the theoretical expression for TRM as function of applied field (adapted from Tauxe 2010):

$$REM = \frac{TRM}{SIRM} = 2REM_s \int_0^{90} \tanh\left(\frac{MB\cos\theta}{kT}\right) \cos\theta \sin\theta d\theta$$



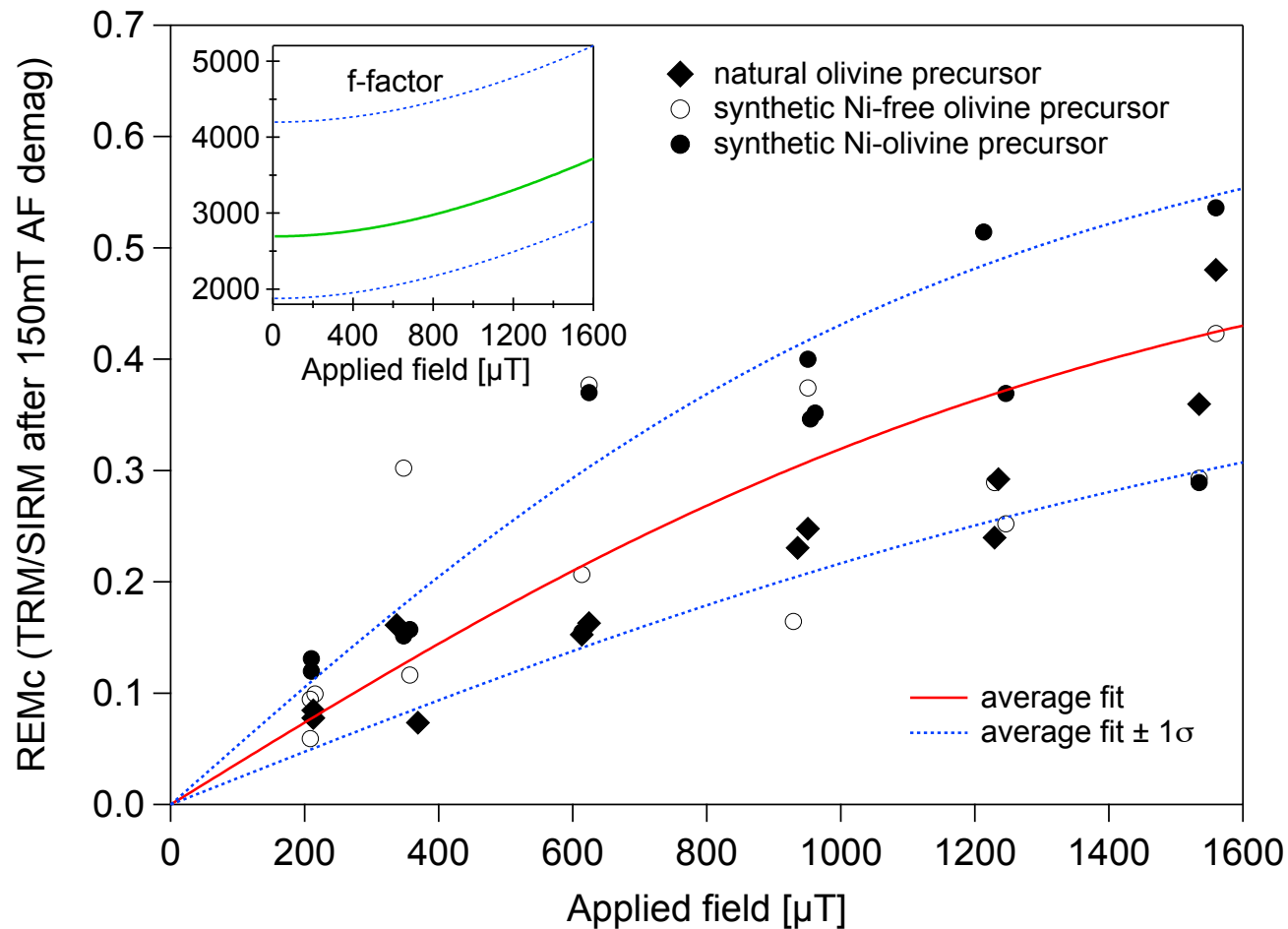
The calibration factor  $f$  is defined so that the magnetising field  $B$  (in  $\mu\text{T}$ ) is equal to  $f \cdot \text{REM}$ . Average  $f$ -factor for REM: 2850

SIRM > saturation TRM  
SV states transform to meta-stable SD states in saturating field  $\rightarrow$  'over normalization'

# Rock-magnetic measurements

## Calibration curve relating applied field to recorded remanence: REMc

REM<sub>c</sub> = TRM left after demag. to 150 mT / IRM left after demag. to 150 mT



Non-linear behavior, average  $f$ -factor: 2695, saturation value: 0.6

Over normalization reduced, more of SD component of remanence is isolated

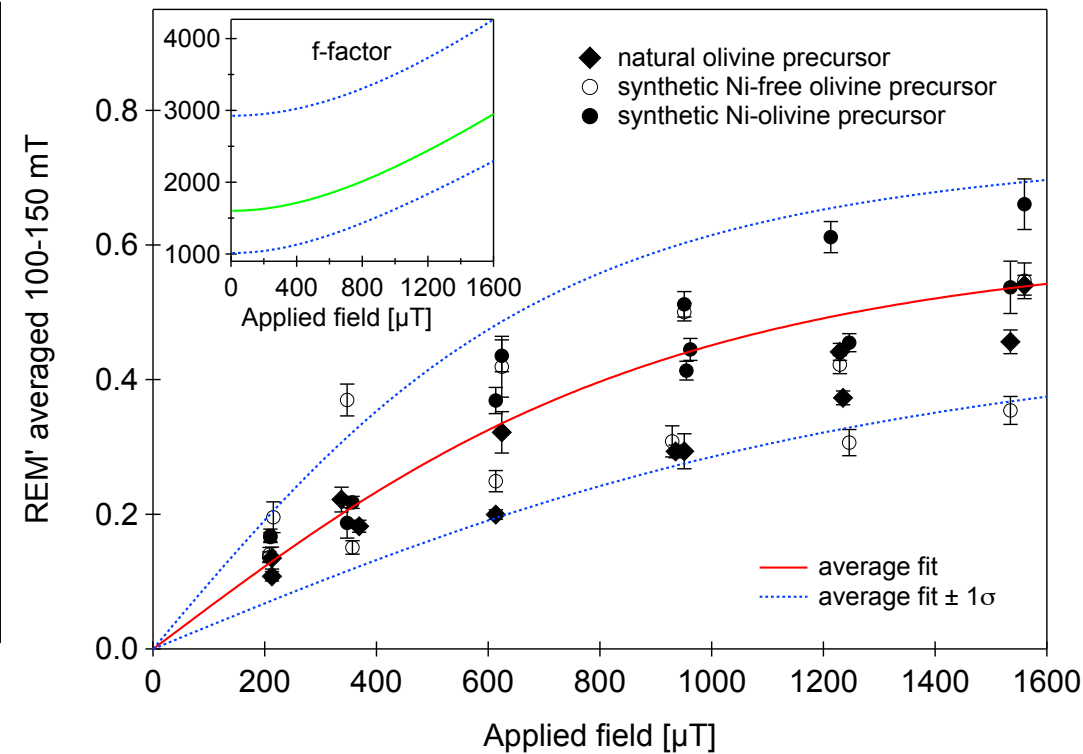
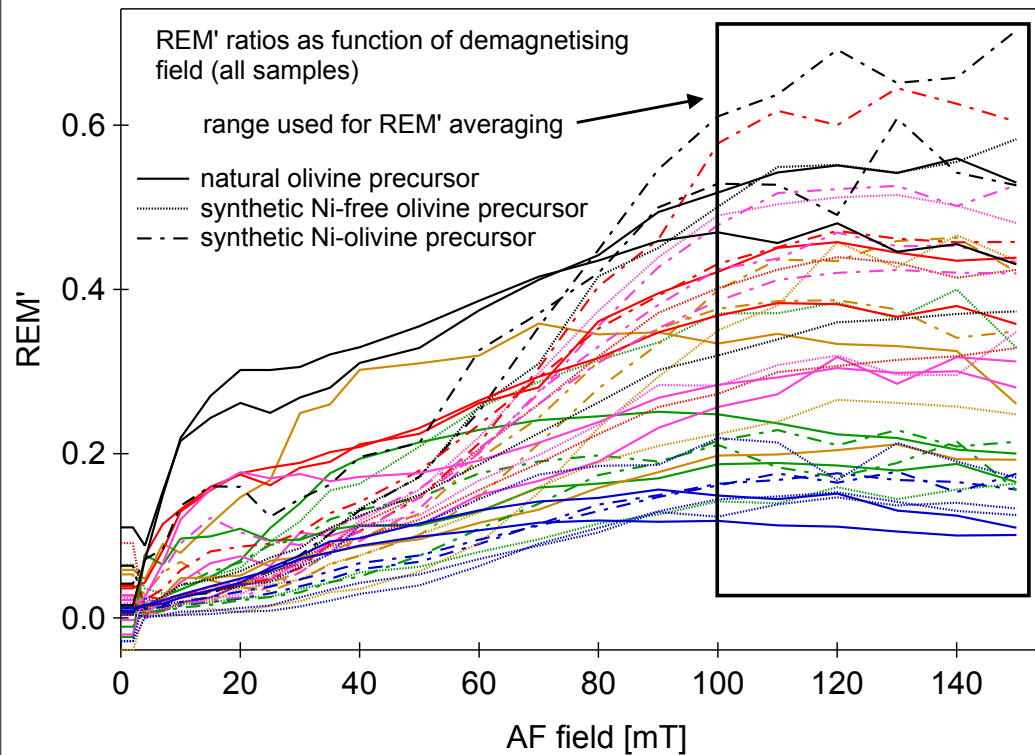
Kletetschka et al. (2003), Gattacceca and Rochette (2004):  $f$ -factor = 3000

# Rock-magnetic measurements

## Calibration curve relating applied field to recorded remanence: REM'

REM' ratio = slope TRM demagnetisation curve/slope IRM demagnetisation curve

$$\text{REM}' = (d\text{TRM}/d\text{AF})/(d\text{IRM}/d\text{AF}) \text{ i.e. } \text{REM}' = (\Delta\text{TRM}/\Delta\text{IRM})$$



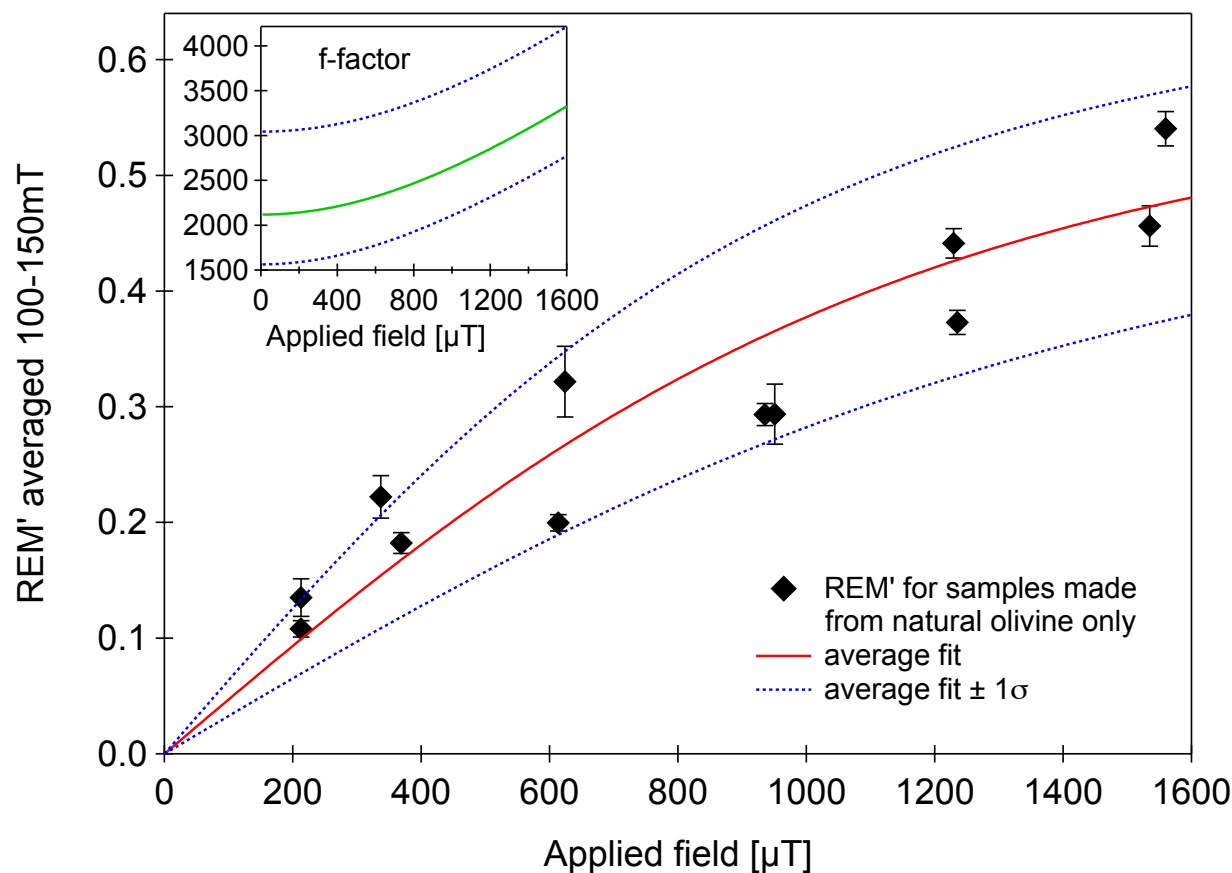
Non-linear behavior, average  $f$ -factor: 1604, saturation value: 0.6

Over normalization reduced, more of SD component of remanence is isolated

Muxworthy et al. (2011):  $f$ -factor = 1900

# Rock-magnetic measurements

## Calibration curve relating applied field to recorded remanence: REM' natural olivine starting material only



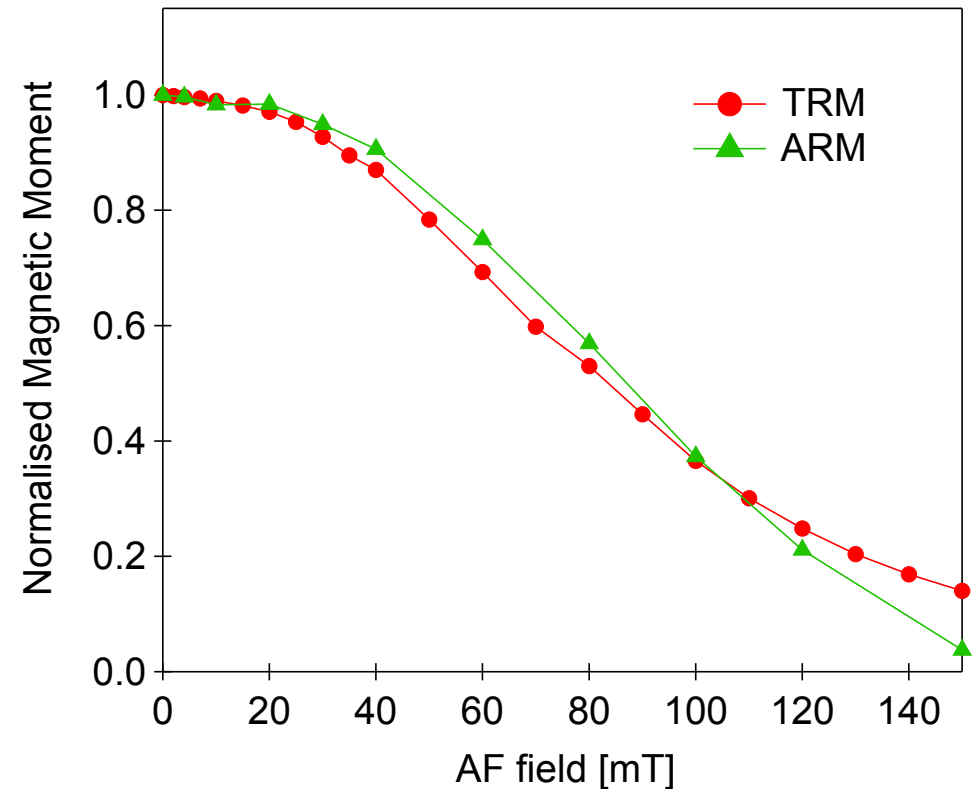
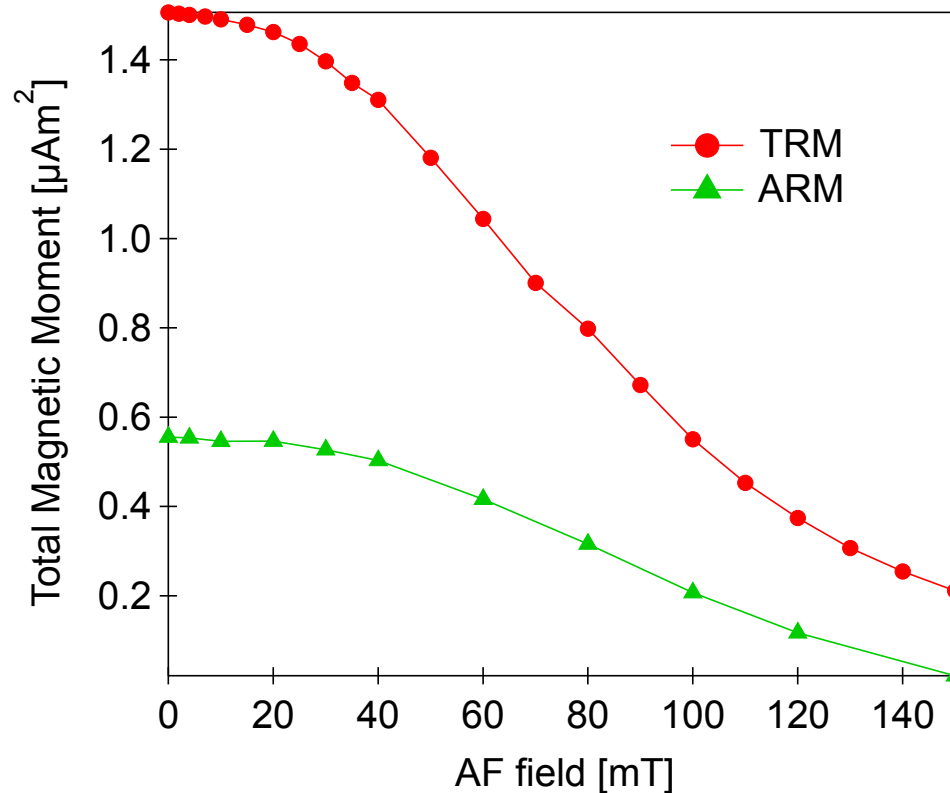
Non-linear behavior, average  $f$ -factor: 2119, saturation value: 0.60

Over normalization reduced, more of SD component of remanence is isolated

Muxworthy et al. (2011):  $f$ -factor = 1900

# Rock-magnetic measurements

## Calibration curve relating applied field to recorded remanence: ARM



AF demagnetisation curve of TRM and ARM are very similar in shape

# Rock-magnetic measurements

---

## Calibration curve relating applied field to recorded remanence: ARM

Relationship between TRM and ARM can be described using the empirical calibration factor  $f_{ARM}$ :

$$f_{ARM} = \frac{\chi_{TRM}}{\chi_{ARM}}$$

$\chi_{TRM}$ ,  $\chi_{ARM}$ : susceptibility of TRM, ARM acquisition

TRM acquired in field  $B_{ancient}$ , ARM acquired in field  $B_{bias}$  in the lab  
 $f_{ARM}$  can be calculated:

$$f_{ARM} = \frac{TRM}{ARM} \frac{B_{bias}}{B_{ancient}} \quad \rightarrow \quad B_{ancient} = \frac{TRM}{ARM} \frac{B_{bias}}{f_{ARM}}$$

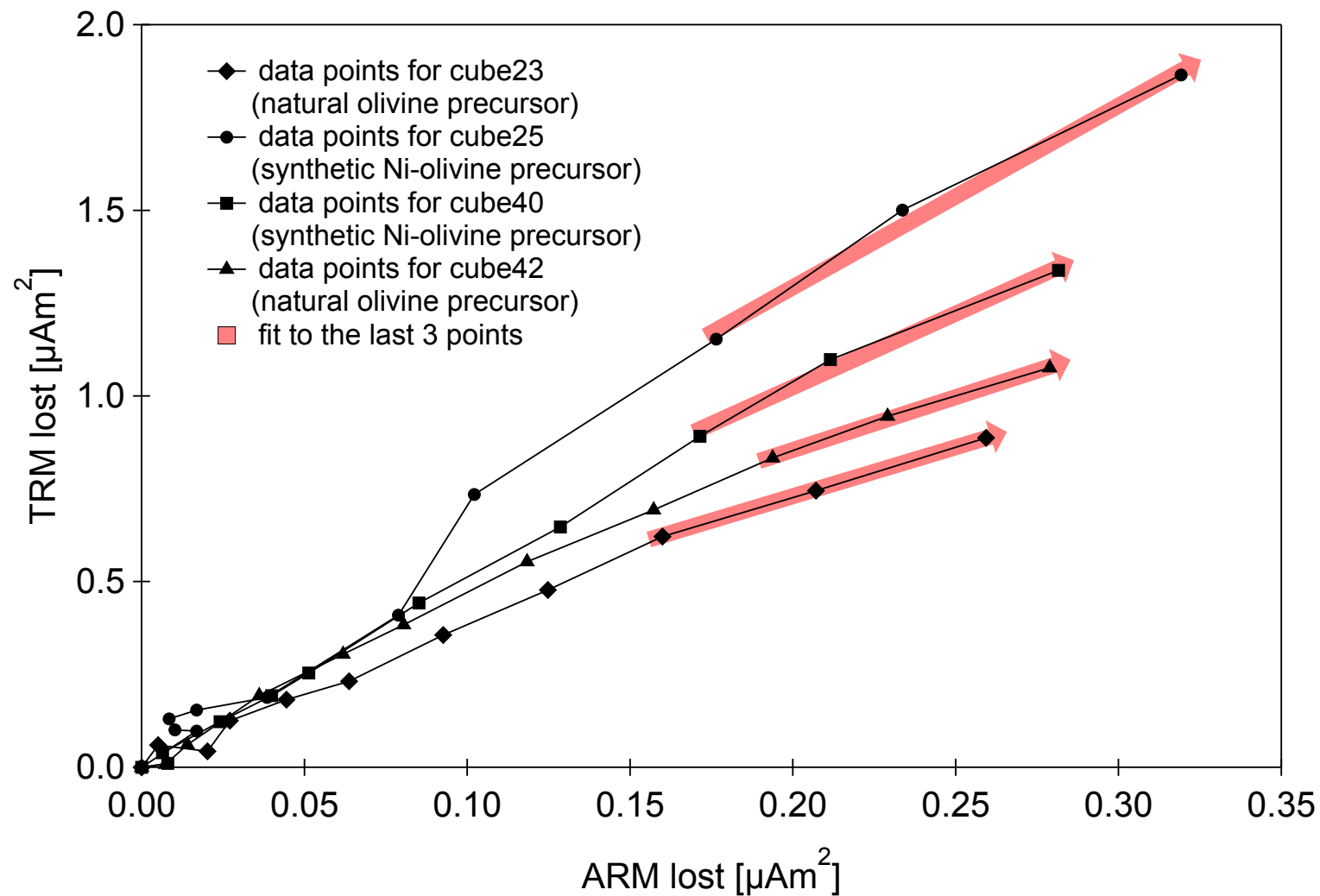
Total remanences TRM, ARM can be substituted by demagnetisation slopes  $dTRM/dAF$  and  $dARM/dAF$ , giving:

$$B_{ancient} = \frac{dTRM}{dARM} \frac{B_{bias}}{f_{ARM}}$$

# Rock-magnetic measurements

## Calibration curve relating applied field to recorded remanence: ARM

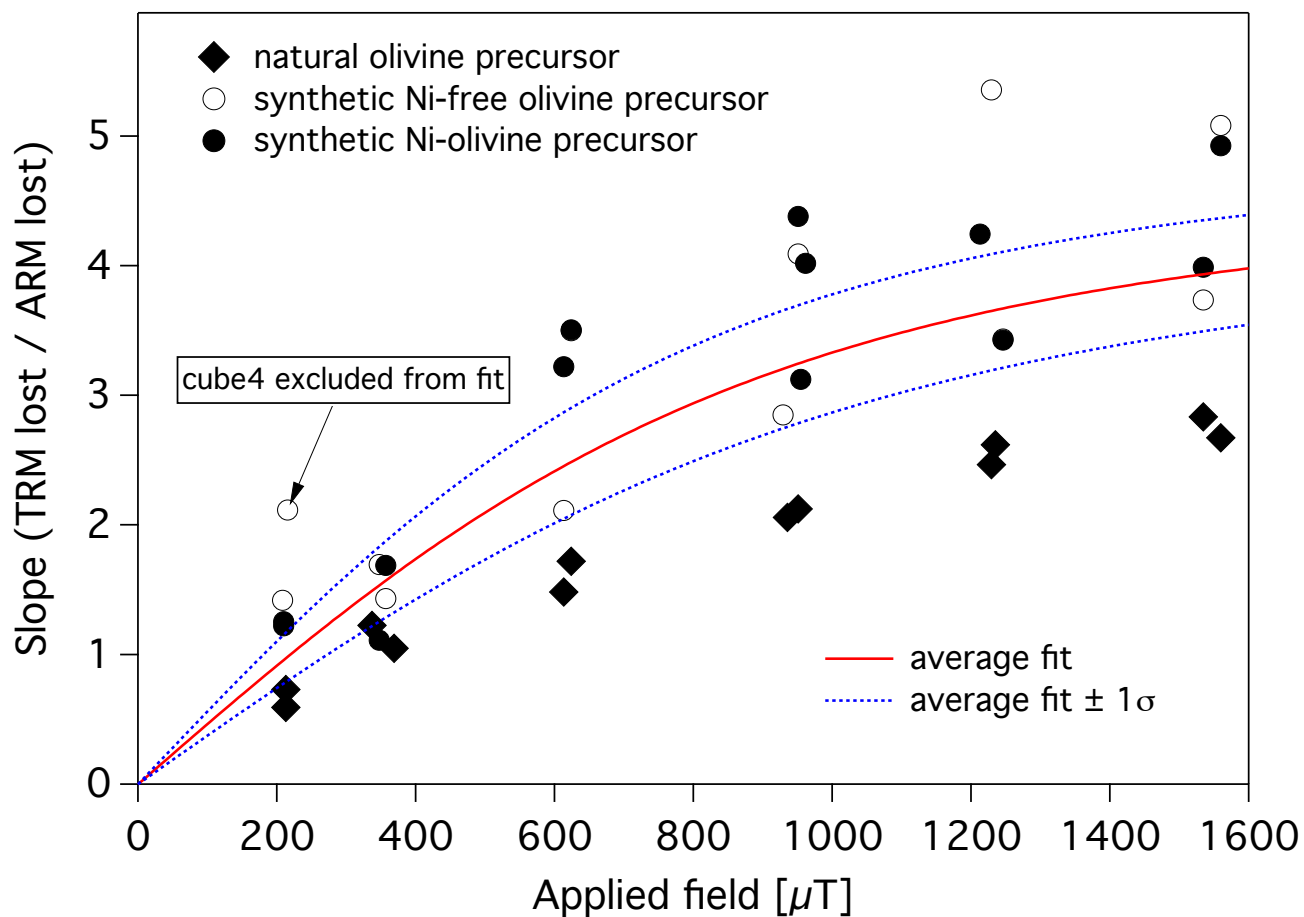
TRM lost at certain point of AF demag vs ARM lost at same demag step



# Rock-magnetic measurements

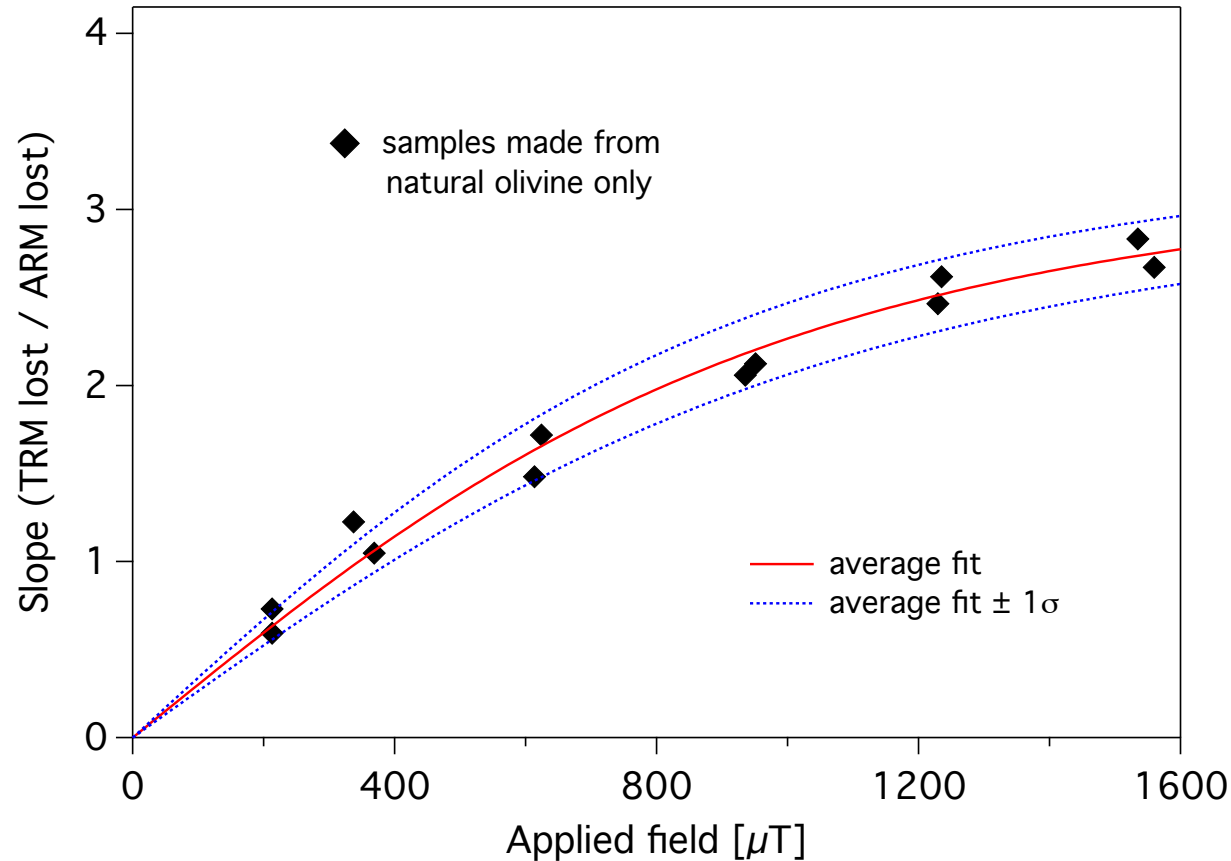
## Calibration curve relating applied field to recorded remanence: ARM

Slope of fit to last 3 points vs applied lab field



# Rock-magnetic measurements

## Calibration curve relating applied field to recorded remanence: ARM natural olivine starting material only

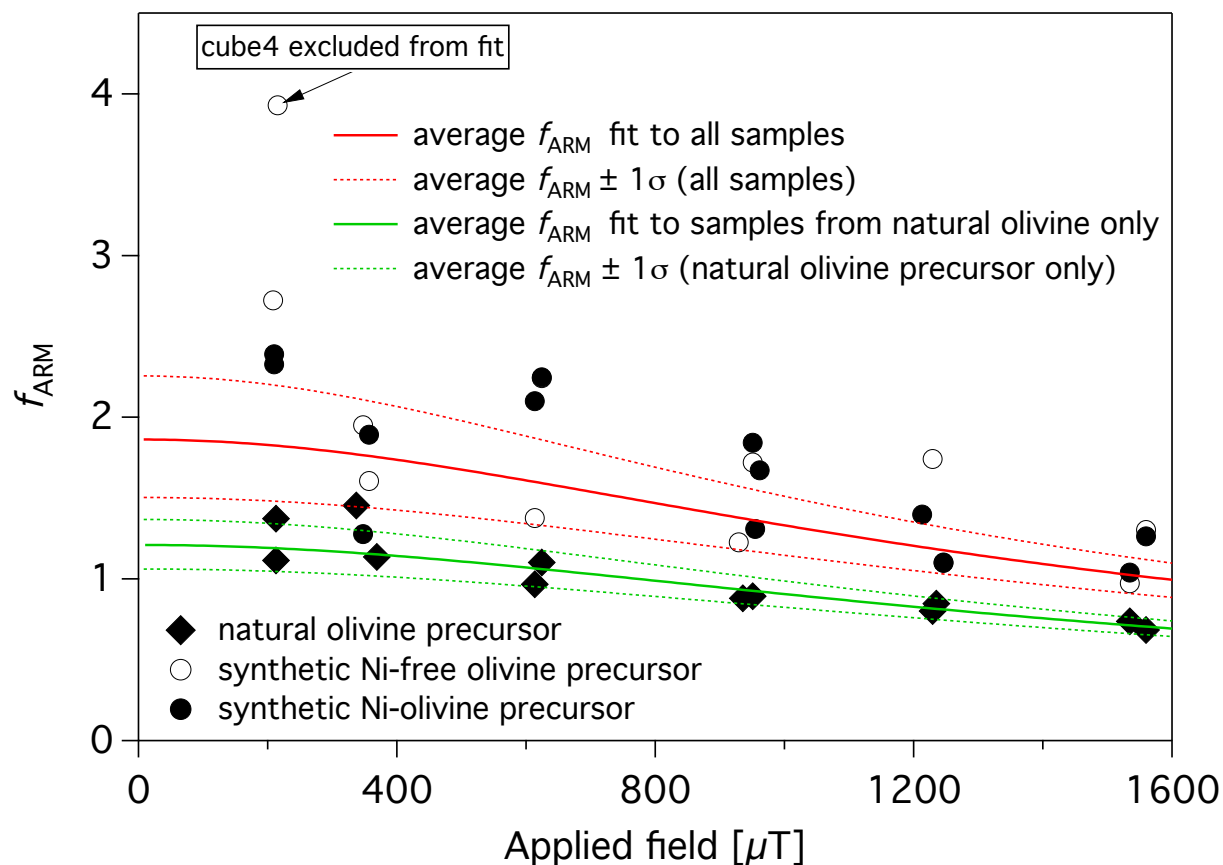


The slope (TRM lost/ARM lost) is specific for the bias field used for the ARM acquisition. Therefore,  $f_{ARM}$  is calculated which is valid generally.

$$f_{ARM} = (\text{slope (TRM lost/ARM lost)} * B_{\text{bias}}) / B_{\text{ancient}}$$

# Rock-magnetic measurements

## Calibration curve relating applied field to recorded remanence: ARM

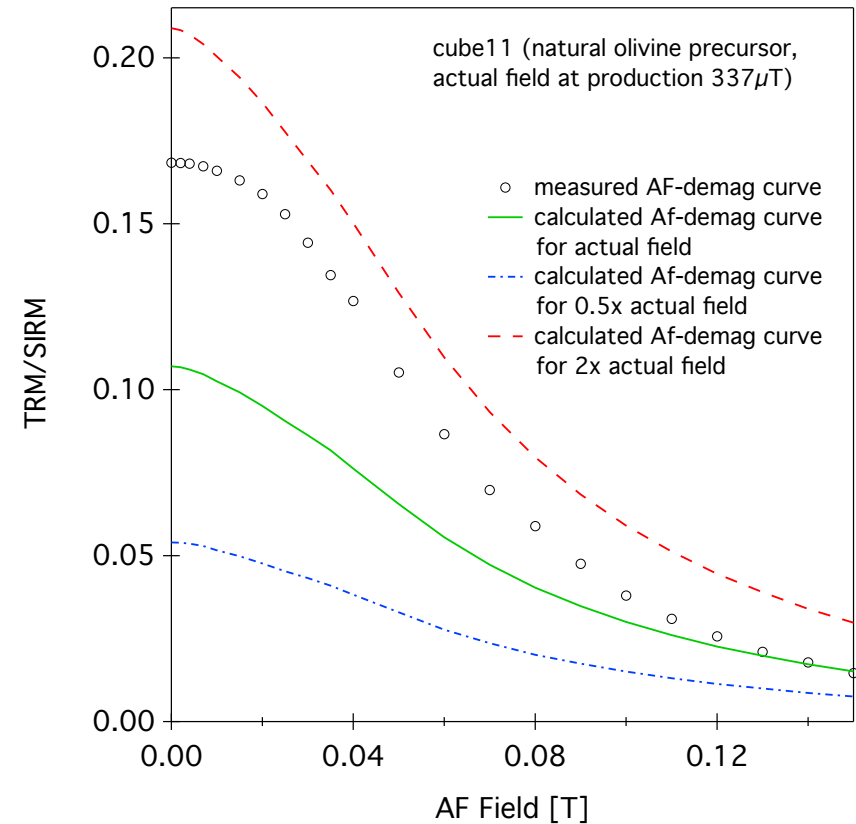
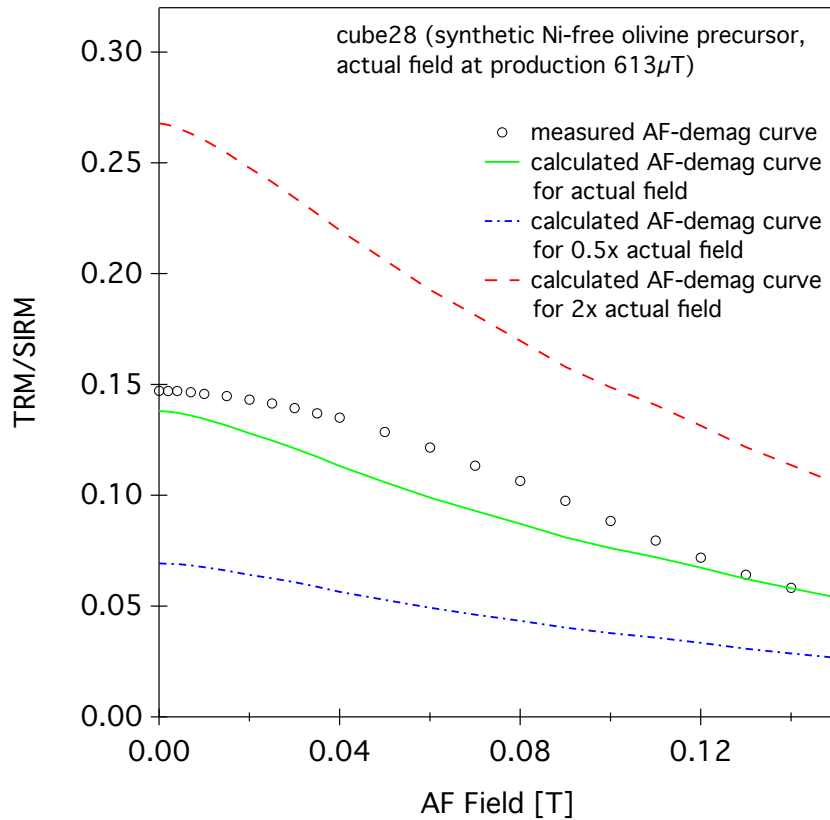


Average  $f_{\text{ARM}}$  at 0 field for all samples: 1.86

Average  $f_{\text{ARM}}$  at 0 field for samples made from natural olivine: 1.21

Yu (2010):  $f_{\text{ARM}} = 2.60 \pm 1.32$

# FORC method

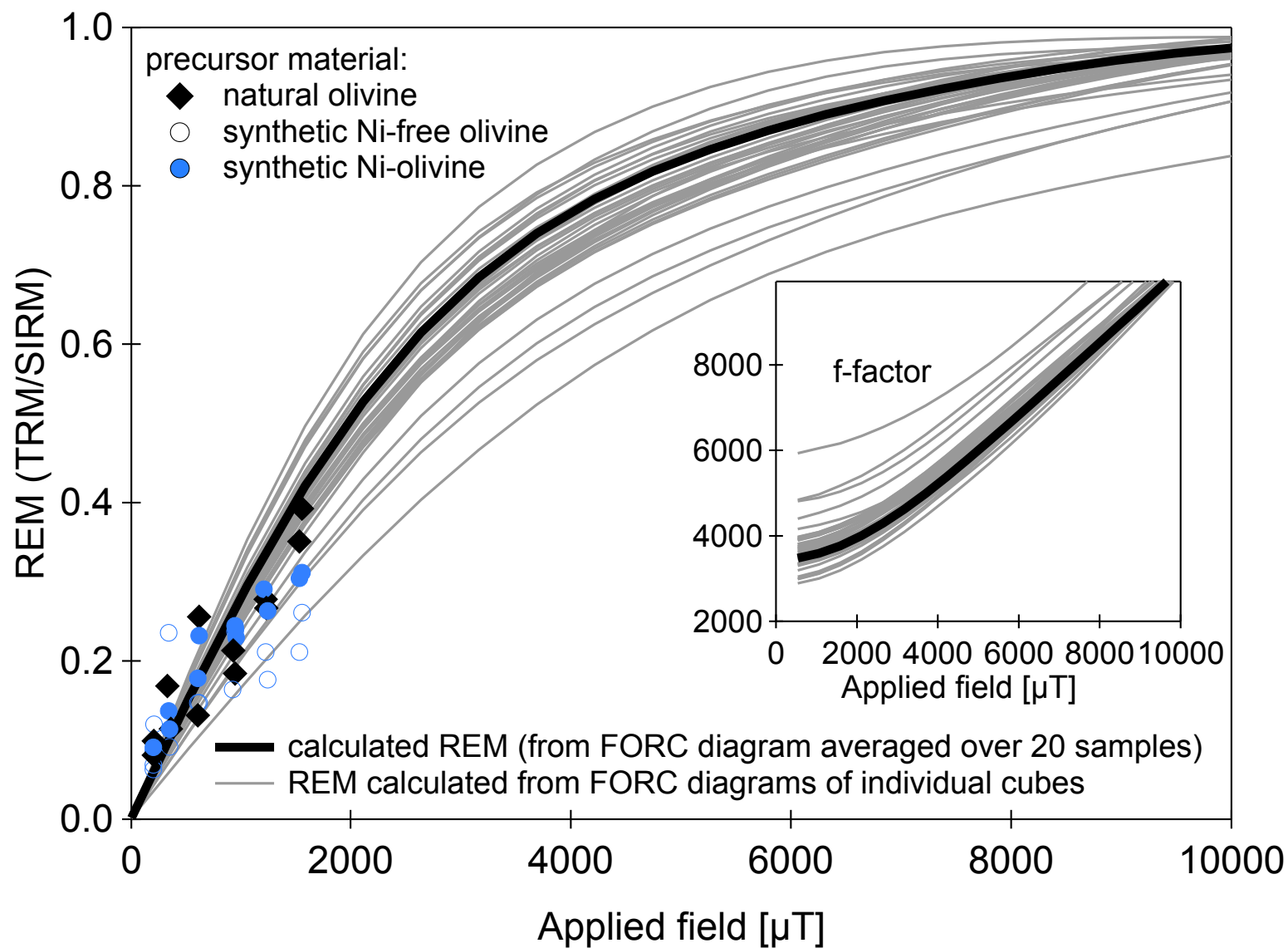


Due to the contribution of vortex states to the FORC signal, the method only works for high demagnetisation fields.

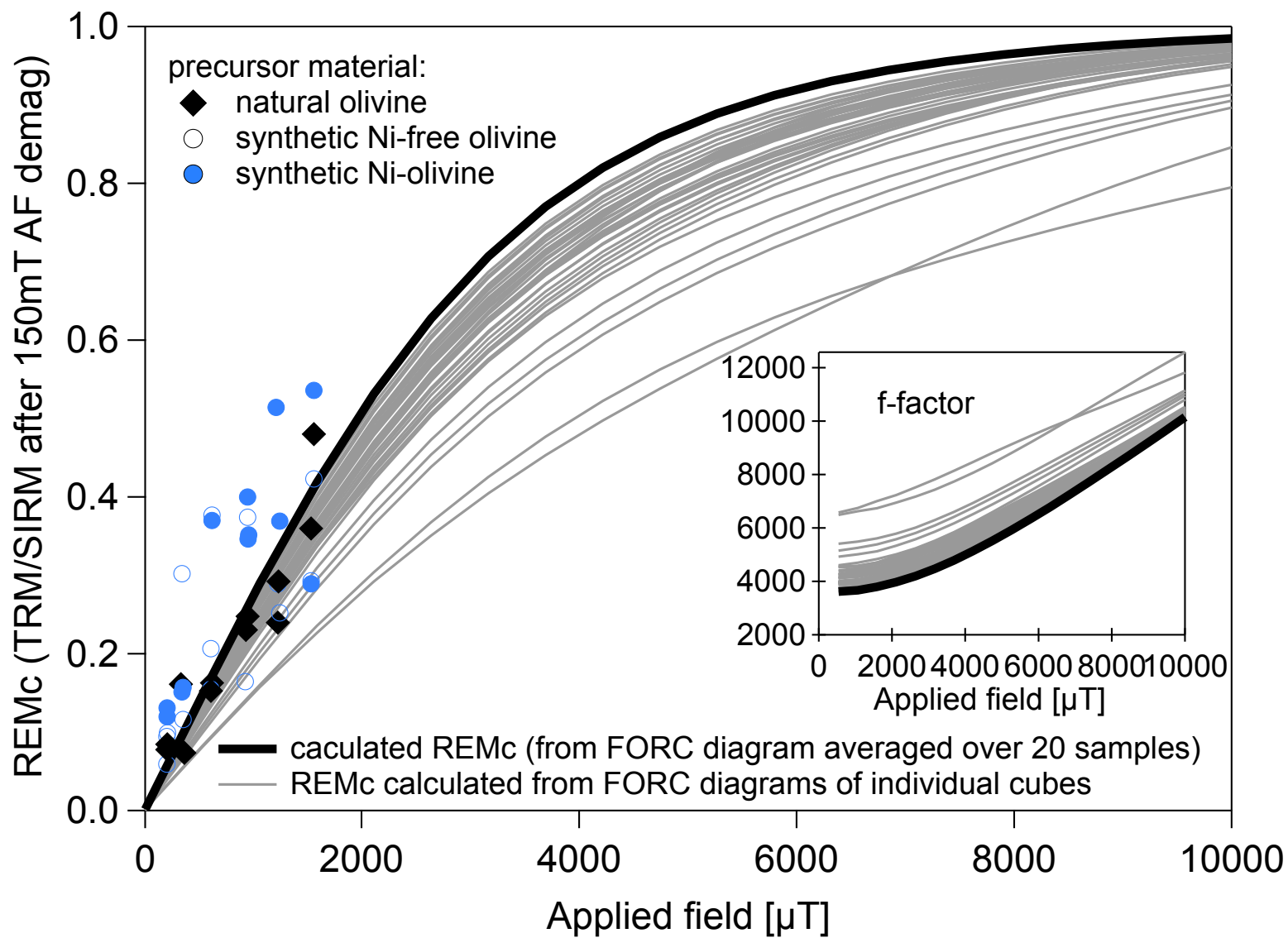
FORC diagrams of samples made from synthetic olivine generally show higher amount of particles in vortex states.

FORC method works best for samples made from natural olivine, which are more SD dominated, at high demagnetisation fields.

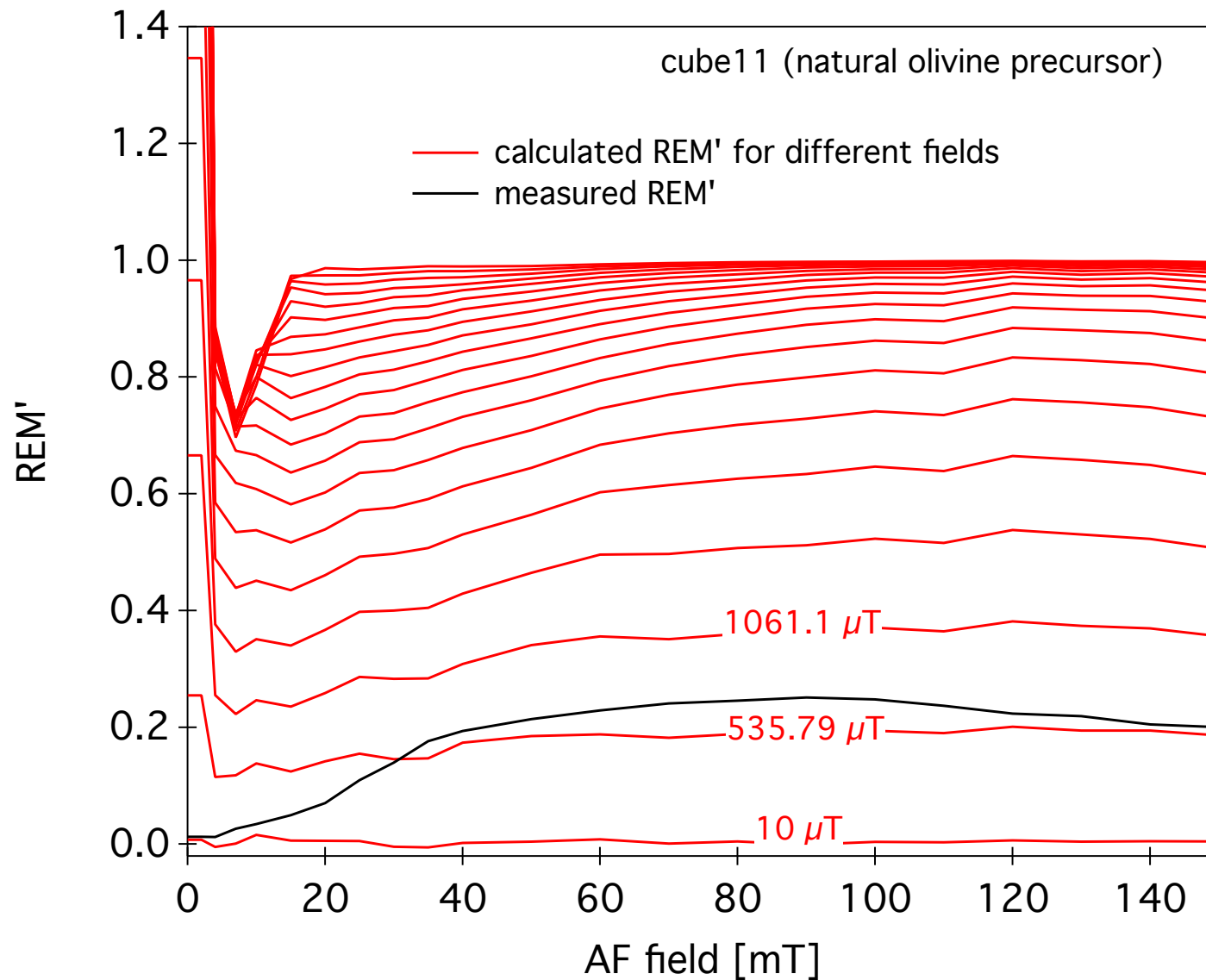
## Calculated REM



## Calculated REMc

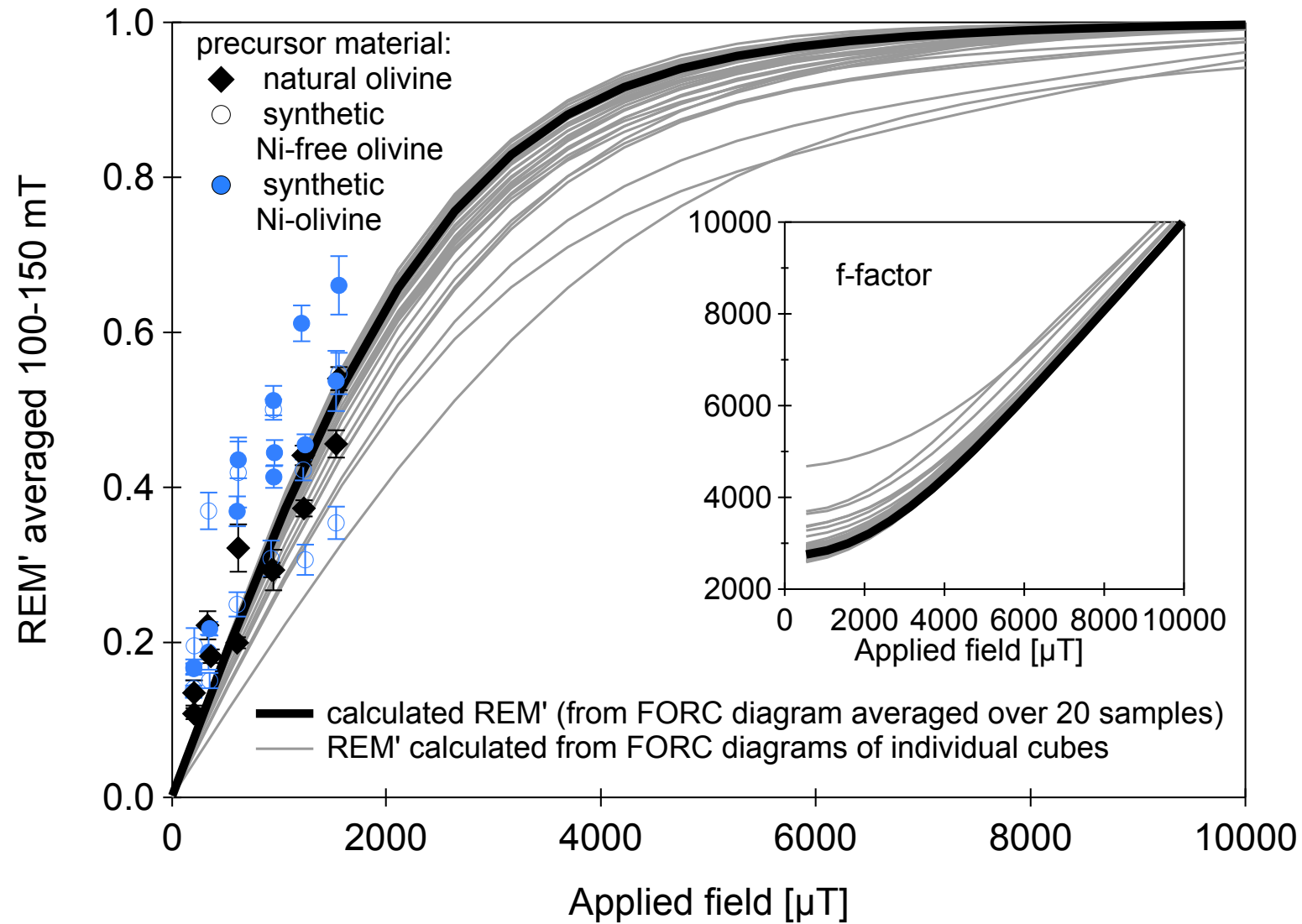


## Calculated REM'



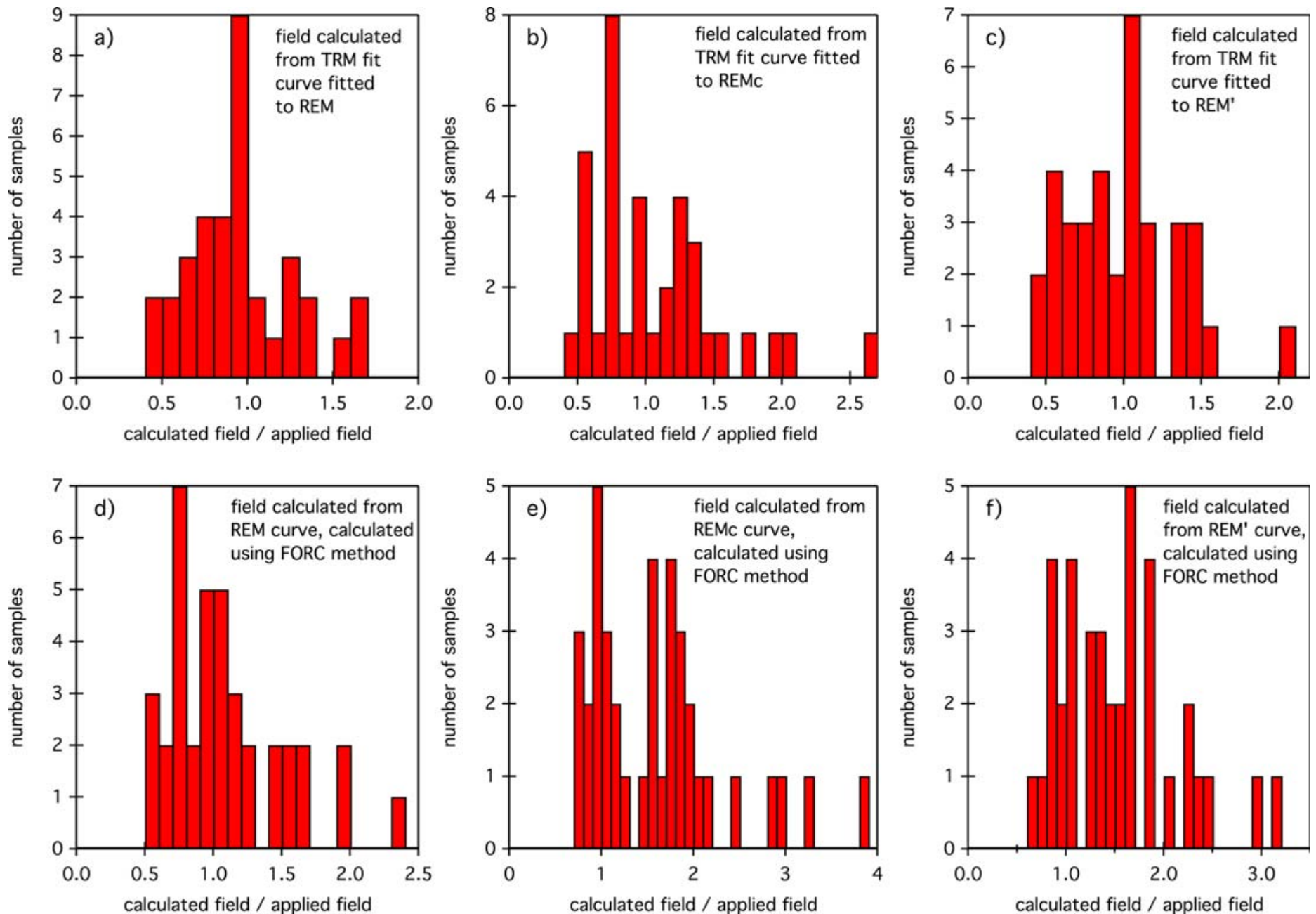
Actual field for  
this sample:  
337  $\mu\text{T}$

## Calculated REM'



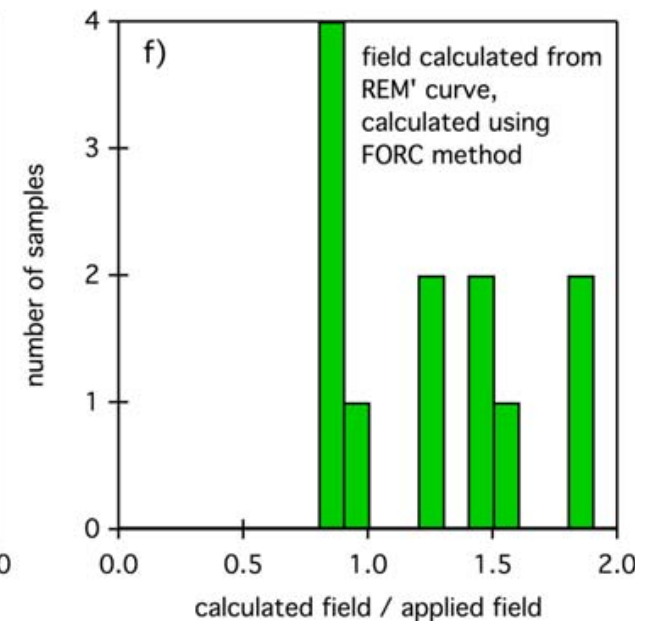
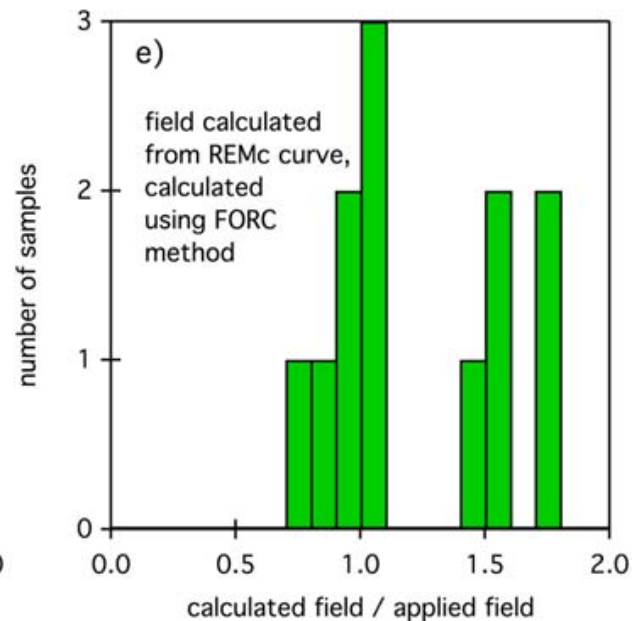
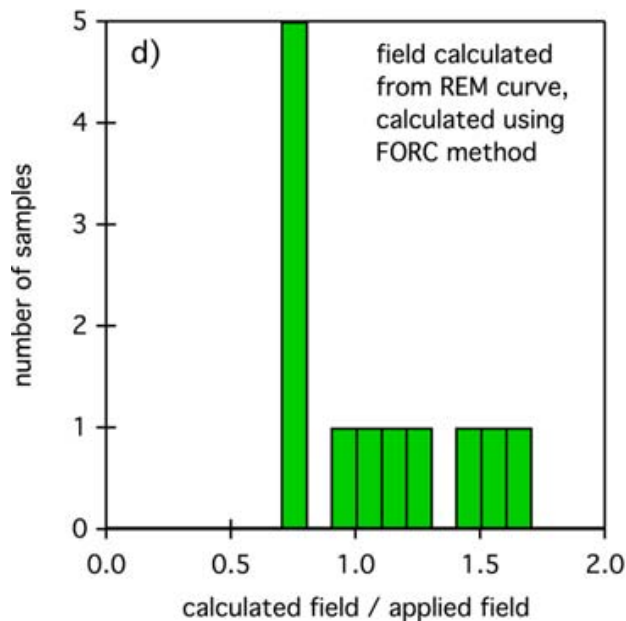
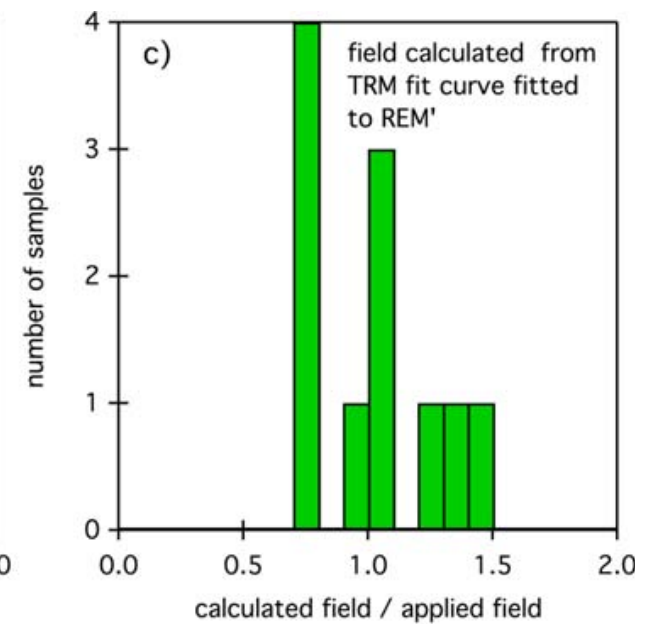
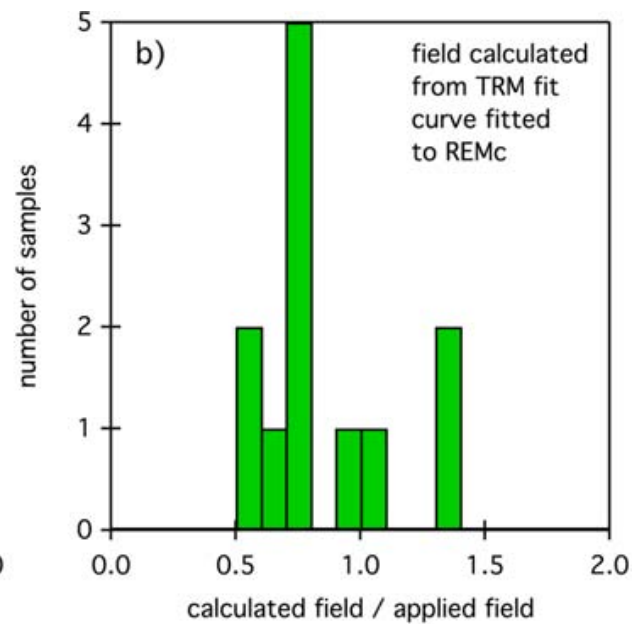
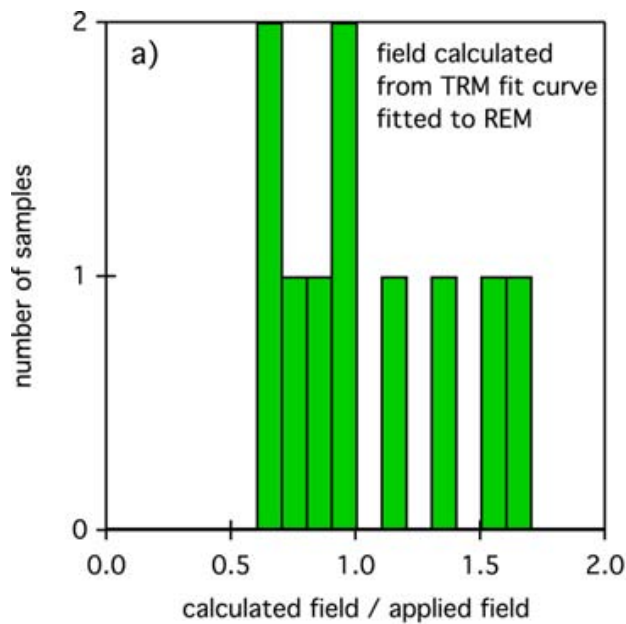
# Rock-magnetic measurements

## Normalized Paleofield Estimates



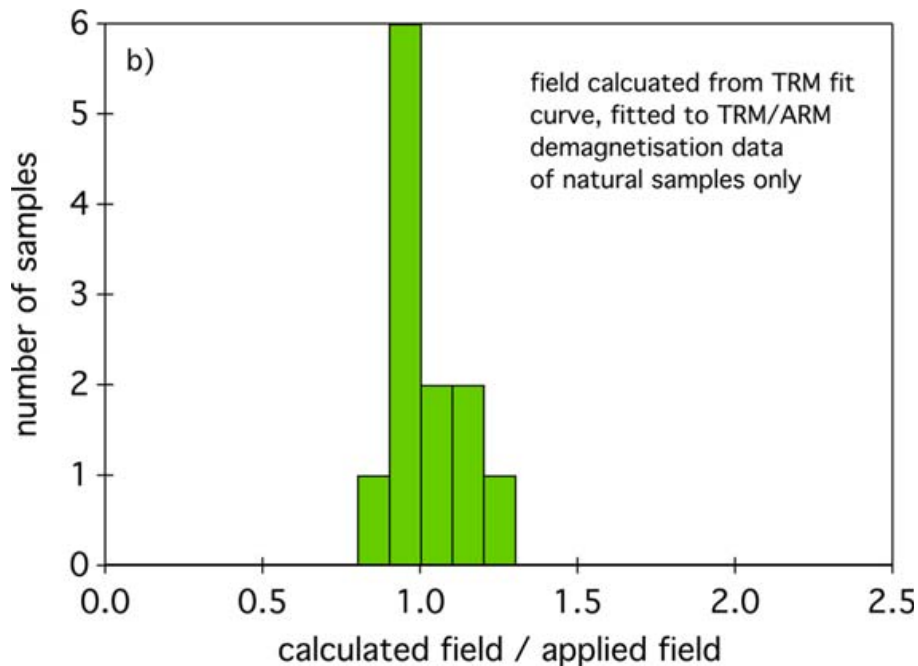
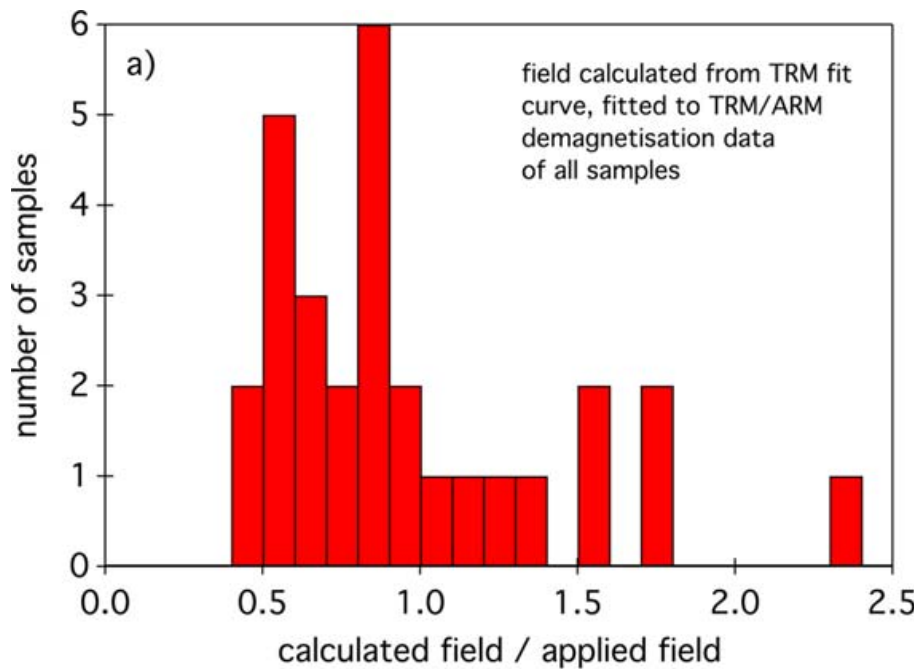
# Rock-magnetic measurements

## Normalized Paleofield Estimates, natural olivine starting material



# Rock-magnetic measurements

## Normalized Paleofield Estimates ARM method



For samples made from natural olivine starting material (i.e. samples dominated by SD particles) the recovered field estimates are within  $\pm 30\%$  of the actual field values

# Conclusions

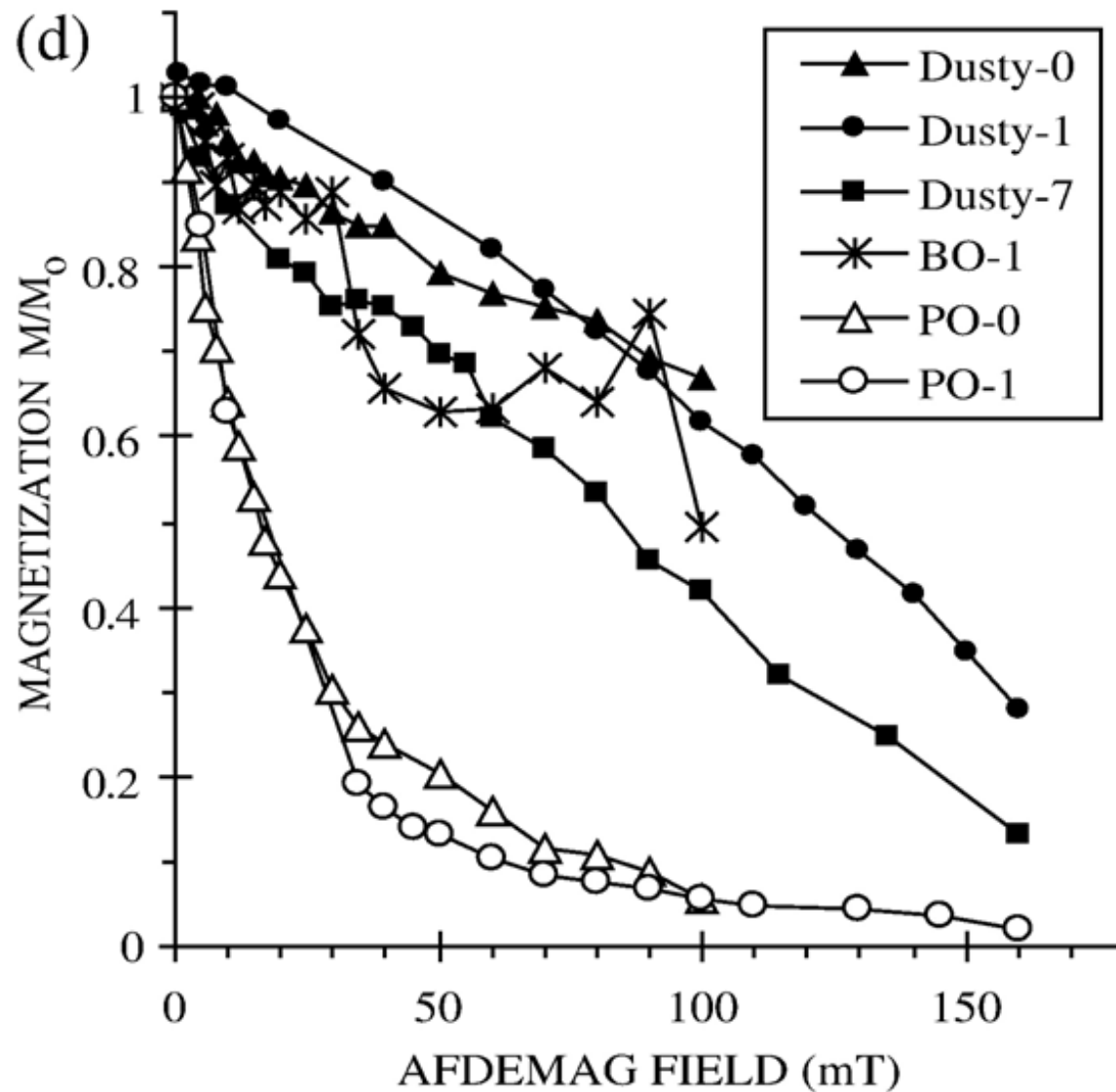
---

- SIRM > saturation TRM due to transformation of SV to metastable SD states → ‘over normalization’ of TRM by SIRM in REM method
- Over normalization reduced in REMc and REM’ method as more of SD component of remanence is isolated
- Data scatter due to variable amounts of SV versus SD particles
- ARM provides closer analogue to TRM than SIRM → ARM normalization of high-coercivity remanence gives best results
- FORC method works well for SD dominated samples, fails for samples with large amounts of SV remanence carriers

**THANK YOU!!**

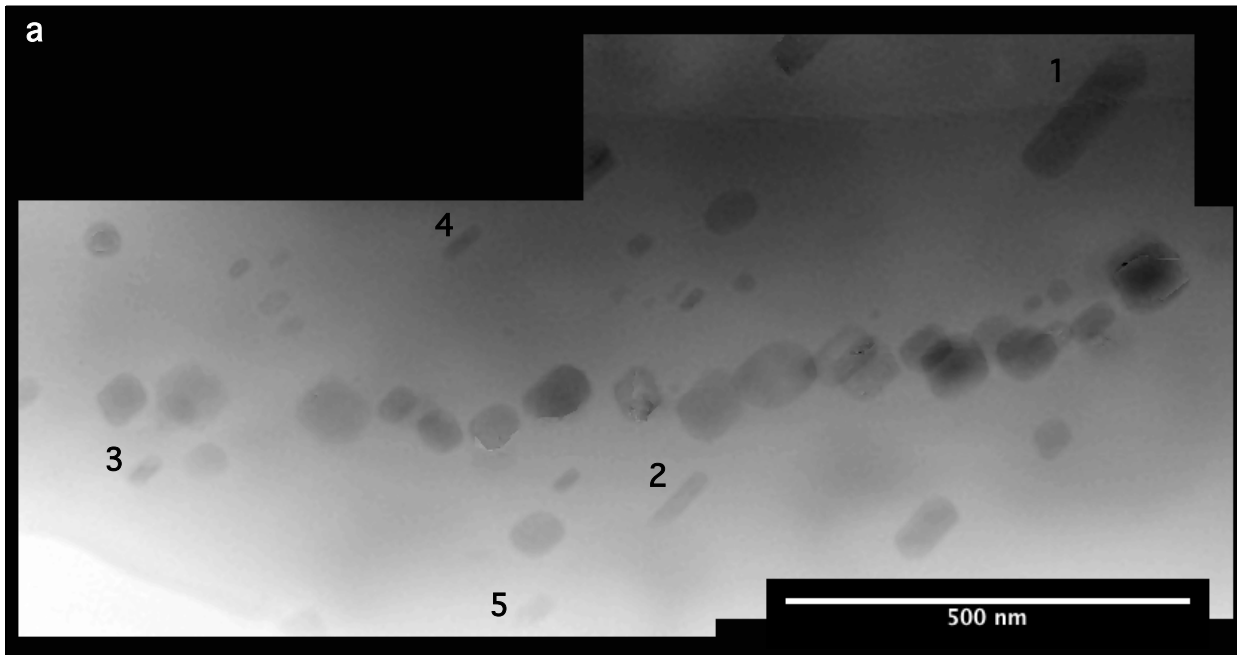
Additional Slides

# Motivation

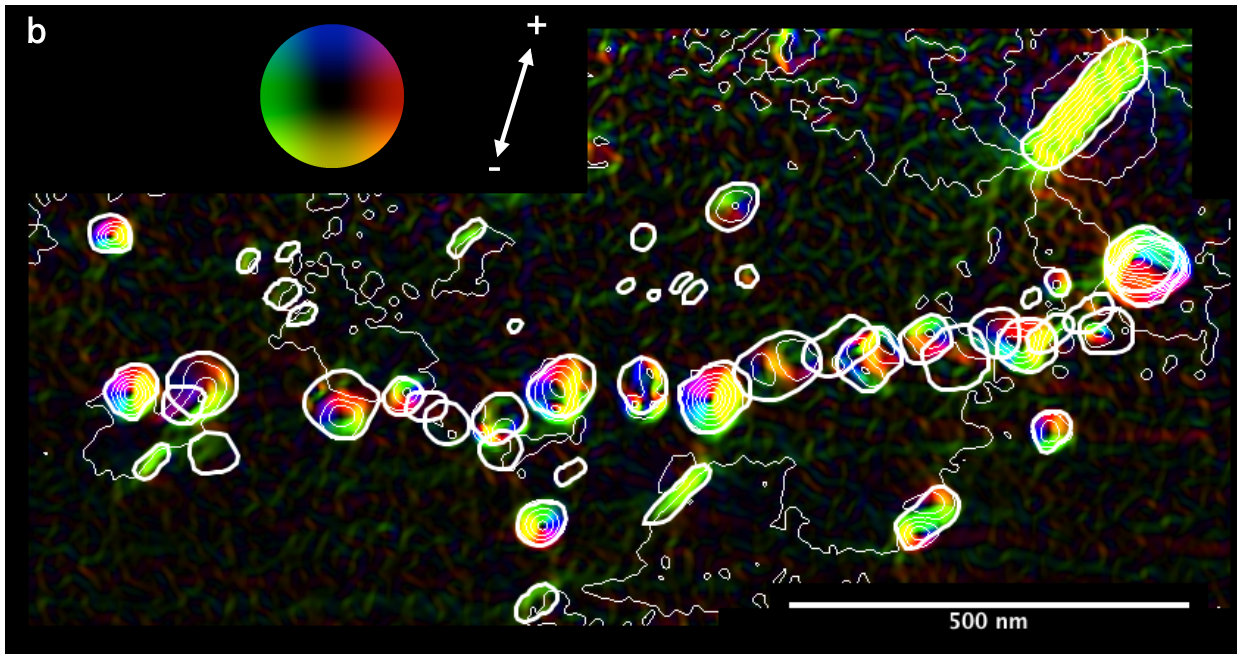


Uehara, M., and N. Nakamura (2006) **Experimental constraints on magnetic stability of chondrules and the paleomagnetic significance of dusty olivine.** *Earth Planet. Sci. Lett.* 250, 292-305, doi: 10.1016/j.epsl.2007.07.002.

# Motivation



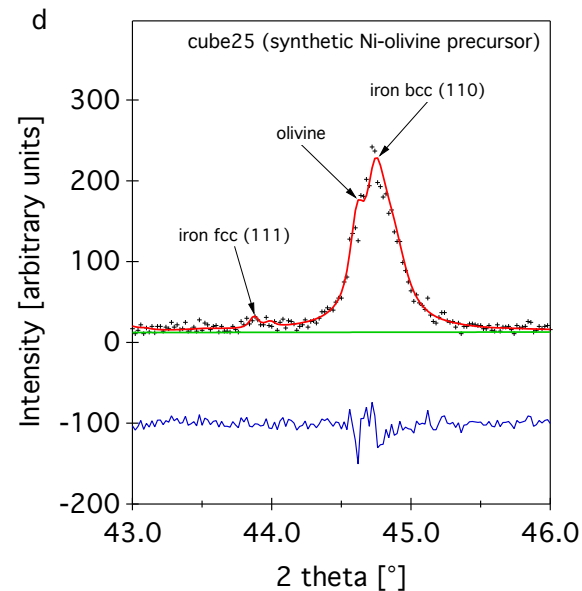
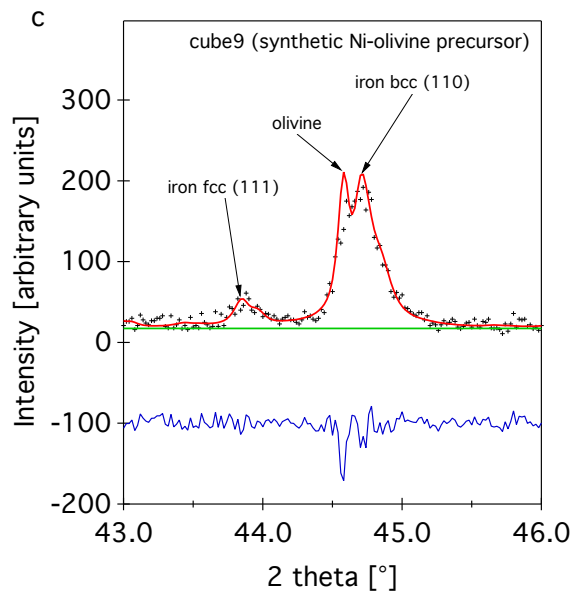
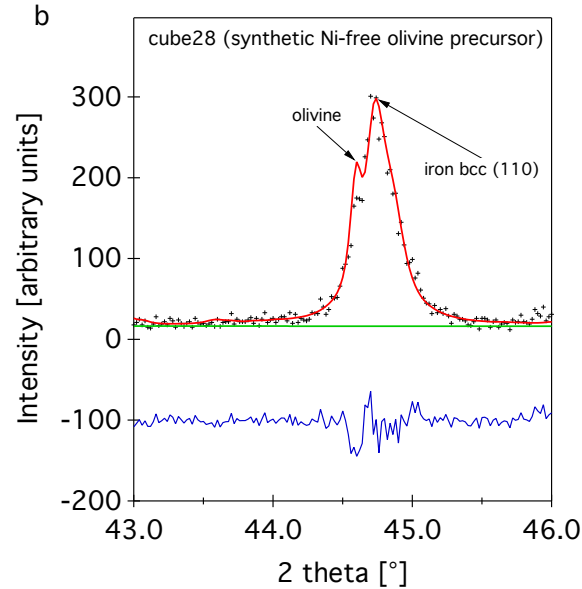
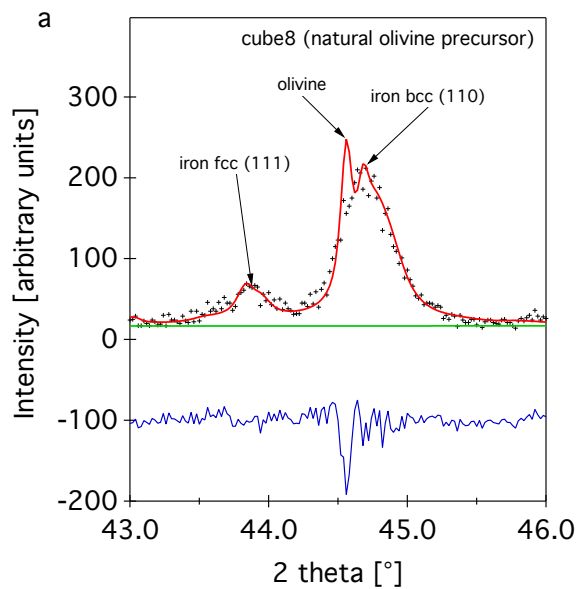
## Synthetic dusty olivine



Lappe, S.-C. L. L., N. S. Church, T. Kasama, A. B. da Silva Fanta, G. Bromiley, R. E. Dunin-Borkowski, J. M. Feinberg, S. Russell, and R. J. Harrison (2011), **Mineral magnetism of dusty olivine: A credible recorder of pre-accretionary remanence**, *Geochem. Geophys. Geosyst.*, 12, Q12Z35, doi:10.1029/2011GC003811.

# Sample characterisation

## X-ray Powder Diffraction



- all samples contain body-centred cubic (bcc) iron
- varying amounts of additional face-centred cubic (fcc) iron

# Sample characterisation

---

## X-ray Powder Diffraction

sample ID	starting material	coherently scattering domain size in bcc-iron [nm]	coherently scattering domain size in fcc-iron [nm]
cube8	natural olivine	$42 \pm 4$	$76 \pm 25$
cube28	synthetic Ni-free olivine	$61 \pm 4$	NA
cube9	synthetic Ni-olivine	$70 \pm 11$	$116 \pm 57$
cube25	synthetic Ni-olivine	$52 \pm 4$	NA

- coherently scattering domain sizes = estimate of grain sizes of Fe
- generally larger for samples made from synthetic olivine
- samples made from synthetic olivine show higher variability in coherently scattering domain sizes for different samples

<b>Calibration method</b>	<b>M[MAm<sup>2</sup>]</b>	<b>REMs</b>	<b>average <math>f</math> factor</b>	<b><math>f</math> factor range</b>
REM	0.0015(5)	0.36(7)	2850 $\mu$ T	1843 < $f$ ( $\mu$ T) < 5038
REMc	0.0010(2)	0.6(1)	2695 $\mu$ T	1877 < $f$ ( $\mu$ T) < 4198
REM'	0.0015(5)	0.6(1)	1604 $\mu$ T	1015 < $f$ ( $\mu$ T) < 2926
REM' natural olivine only	0.0012(2)	0.60(7)	2119 $\mu$ T	1564 < $f$ ( $\mu$ T) < 3044
<b>Calibration method</b>	<b>M[MAm<sup>2</sup>]</b>	<b>dTRM/dARMs</b>	<b>average <math>f_{\text{ARM}}</math> at 0 field</b>	<b><math>f_{\text{ARM}}</math> range at 0 field</b>
ARM	0.0015(2)	4.6(3)	1.86	1.50 < $f_{\text{ARM}}$ < 2.26
ARM natural olivine only	0.0014(1)	3.3(1)	1.21	1.06 < $f_{\text{ARM}}$ < 1.37

